frontiers in Physiology

ORIGINAL RESEARCH
published: 19 August 2021
doi: 10.3389/fphys.2021.582037

The Functional Role of Hyperpolarization Activated Current (I_f) on Cardiac Pacemaking in Human vs. in the Rabbit Sinoatrial Node: A Simulation and Theoretical Study

Xiangyun Bai[1,2,3], *Kuanquan Wang*[3], *Mark R. Boyett*[4], *Jules C. Hancox*[1,5] *and Henggui Zhang*[1,6,7*]

[1] Biological Physics Group, Department of Physics and Astronomy, The University of Manchester, Manchester, United Kingdom, [2] School of Computer Science and Technology, Xi'an University of Posts and Telecommunications, Xi'an, China, [3] School of Computer Science and Technology, Harbin Institute of Technology, Harbin, China, [4] Department of Biomedical Sciences, Faculty of Health and Medical Sciences, University of Copenhagen, København, Denmark, [5] School of Physiology, Pharmacology and Neuroscience, Biomedical Sciences Building, University Walk, Bristol, United Kingdom, [6] Peng Cheng Laboratory, Shenzhen, China, [7] Key Laboratory of Medical Electrophysiology of Ministry of Education, Medical Electrophysiological Key Laboratory of Sichuan, Institute of Cardiovascular Research, Southwest Medical University, Luzhou, China

OPEN ACCESS

Edited by:
Gerard J. J. Boink,
University of Amsterdam, Netherlands

Reviewed by:
Thomas Hund,
The Ohio State University, United States
Victor A. Maltsev,
National Institute on Aging (NIH), United States

***Correspondence:**
Henggui Zhang
henggui.zhang@manchester.ac.uk

Specialty section:
This article was submitted to Computational Physiology and Medicine, a section of the journal Frontiers in Physiology

Received: 10 July 2020
Accepted: 23 July 2021
Published: 19 August 2021

Citation:
Bai X, Wang K, Boyett MR, Hancox JC and Zhang H (2021) The Functional Role of Hyperpolarization Activated Current (I_f) on Cardiac Pacemaking in Human vs. in the Rabbit Sinoatrial Node: A Simulation and Theoretical Study. Front. Physiol. 12:582037. doi: 10.3389/fphys.2021.582037

The cardiac hyperpolarization-activated "funny" current (I_f), which contributes to sinoatrial node (SAN) pacemaking, has a more negative half-maximal activation voltage and smaller fully-activated macroscopic conductance in human than in rabbit SAN cells. The consequences of these differences for the relative roles of I_f in the two species, and for their responses to the specific bradycardic agent ivabradine at clinical doses have not been systematically explored. This study aims to address these issues, through incorporating rabbit and human I_f formulations developed by Fabbri et al. into the Severi et al. model of rabbit SAN cells. A theory was developed to correlate the effect of I_f reduction with the total inward depolarising current (I_{total}) during diastolic depolarization. Replacing the rabbit I_f formulation with the human one increased the pacemaking cycle length (CL) from 355 to 1,139 ms. With up to 20% I_f reduction (a level close to the inhibition of I_f by ivabradine at clinical concentrations), a modest increase (~5%) in the pacemaking CL was observed with the rabbit I_f formulation; however, the effect was doubled (~12.4%) for the human I_f formulation, even though the latter has smaller I_f density. When the action of acetylcholine (ACh, 0.1 nM) was considered, a 20% I_f reduction markedly increased the pacemaking CL by 37.5% (~27.3% reduction in the pacing rate), which is similar to the ivabradine effect at clinical concentrations. Theoretical analysis showed that the resultant increase of the pacemaking CL is inversely proportional to the magnitude of I_{total} during diastolic depolarization phase: a smaller I_f in the model resulted in a smaller I_{total} amplitude, resulting in a slower pacemaking rate; and the same reduction in I_f resulted in a more significant change of CL in the cell model with a smaller I_{total}. This explained the mechanism by which a low dose of ivabradine slows pacemaking

rate more in humans than in the rabbit. Similar results were seen in the Fabbri et al. model of human SAN cells, suggesting our observations are model-independent. Collectively, the results of study explain why low dose ivabradine at clinically relevant concentrations acts as an effective bradycardic agent in modulating human SAN pacemaking.

Keywords: human and rabbit sinoatrial node, funny current, bradycardic agent (ivabradine), electrophysiological simulation, theoretical analysis

INTRODUCTION

The pacemaker activity of sinoatrial node (SAN) cells in the mammalian heart arises from the integrated action of multiple sarcolemmal ionic channel currents and the interaction between the intracellular calcium handling and sarcolemmal electrogenic processes (Irisawa et al., 1993; Mangoni and Nargeot, 2008; Lakatta et al., 2010). The hyperpolarization-activated "funny" current, I_f, present in the SAN and other regions of the cardiac conduction system (Boyett, 2009; Difrancesco, 2010), is produced by the hyperpolarization-activated cyclic nucleotide gated (HCN) channel isoforms (of which there are four: HCN1-4), each of which is comprised of six transmembrane domains with four subunits combining to produce functional tetrameric channels, as occurs for voltage-gated potassium channels (Bois et al., 2007; Difrancesco, 2010). Previous studies of the rabbit SAN have shown that although HCN isoforms 1, 2, and 4 are all expressed in the heart, HCN4 is the most abundant in the SAN and the I_f density within SAN sub-regions correlates strongly with HCN4 expression levels (Thollon et al., 2007; Brioschi et al., 2009). The unique features of HCN channels lie in the fact that they are activated not on depolarization but on hyperpolarization of cell membrane potential (to voltages negative to ∼−40 to ∼−50 mV) (Hagiwara and Irisawa, 1989; Accili et al., 1997; Baruscotti et al., 2005) and are permeable to both Na^+ and K^+ ions, with an approximate reversal potential of −30 mV (Van Ginneken and Giles, 1991; Verkerk et al., 2009a). Upon hyperpolarization, HCN channels generate an inward current over the pacemaking potential range which, together with the current generated by other electrogenic processes of the intracellular calcium handling (i.e., the Ca^{2+} clock), contributes to the genesis of intrinsic pacemaker activity of the SAN (Lakatta and Difrancesco, 2009). HCN channels are also modulated by adrenergic agonists *via* cAMP (Bucchi et al., 2003; Craven and Zagotta, 2006).

I_f channels are also present in the human SAN. It has been shown that HCN4 is strongly expressed in the human SAN, with the measured mRNA level of other isoforms accounting for <16% (with HCN3 being negligible, accounting for only 0.5%) of the total mRNA measurement (Chandler et al., 2009). Though the HCN expression in the human SAN is similar to that in the rabbit, properties and kinetics of I_f are clearly different. It has been shown the fully-activated I_f conductance in the human is about 3–4 times smaller than that in the rabbit (Verkerk et al., 2007a). Additionally, I_f in human SAN cells has a more negative half-maximal activation voltage, and a greater time constant of deactivation/activation process which is also negatively shifted (Verkerk et al., 2007a). With such a marked species differences in I_f conductance and kinetics between the rabbit and human, a question arises as to whether a smaller I_f in the human SAN cells plays the same important role in regulating cardiac pacemaking activity as in the rabbit SAN?

Although I_f in human SAN cells is much smaller than those in other mammals, it may play a comparable role to that in the rabbit in modulating cardiac pacemaking. In their study, (Verkerk et al., 2007b) observed about a 26% increase in pacemaking cycle length in human SAN cells on complete block of I_f by using 2 mM Cs^+, which is close to that seen in the rabbit (Verkerk and Wilders, 2010; Fabbri et al., 2017). Pharmacological targeting of I_f by ivabradine has also shown the clinical value of I_f in controlling the heart rate in patients who need heart rate control in conditions of coronary artery disease (CAD) (Tardif et al., 2005; Camici et al., 2016; Niccoli et al., 2017) and heart failure (HF) (Bohm et al., 2015; Yancy et al., 2016). In both conditions, slowing down the heart rate by ivabradine increases the diastolic interval, thereby reducing the metabolic load on the working myocardium; this reduces the risks of ischemia of the heart leading to reduced risk of sudden death (Niccoli et al., 2017).

Although inhibition of I_f by ivabradine provides an efficient pharmacological control of heart rate in the clinic, it is still unclear how the clinical concentration range of ivabradine [about 20–140 nM (Choi et al., 2013; Jiang et al., 2013); blocking I_f < 20% (Bois et al., 1996; Bucchi et al., 2002)] can produce a significant effect in reducing human heart rate. In pre-clinical animal model studies, ivabradine has been reported to inhibit I_f in SAN cells with a half-maximal inhibitory concentration of 1.5–2.8 μM (Bois et al., 1996; Bucchi et al., 2002), and recombinant HCN4 channels with an IC_{50} values between 0.5 and 2.0 μM (Bucchi et al., 2002, 2006, 2013). In rabbit SAN cells, 1 μM ivabradine has been observed to reduce the pacemaking rate by 12.3% (Thollon et al., 1994), whilst about 16.2 and 23.8% of heart rate reduction at 3 μM have been seen (Thollon et al., 1994; Bucchi et al., 2007).

When ivabradine was administered intravenously (0.2 mg kg^{-1}) to patients with normal baseline electrophysiology, mean heart rate reductions of 12.9 and 14.1 beats min^{-1} (at 0.5 and 1 h respectively following administration) were observed (Camm and Lau, 2003). The drug is usually administered orally, however, and after repeated oral dosing at 5 mg, mean maximal plasma (C_{max}) levels of 11–16 ng ml^{-1} (23.5–34.1 nM) have been measured, whilst for repeated dosing at 10 mg, mean C_{max} levels of 29–42 ng ml^{-1} (61.8–89.6 nM) have been seen (Choi et al., 2013; Jiang et al., 2013).

Repeated dosing with a high ivabradine concentration of 20 mg has been associated with a C_{max} of 137 nM (Jiang et al., 2013). On the basis of the pre-clinically observed concentration-dependence for I_f inhibition, comparatively low levels of I_f block might be expected at such plasma levels (Thollon et al., 1994; Bucchi et al., 2007). However, clinical concentrations of ivabradine produce about 18–20% reduction in human heart rate (Camm and Lau, 2003; Doesch et al., 2007).

Previous animal model studies (Difrancesco, 1991, 2010) have found that inhibition of I_f by ivabradine slowed down the spontaneous firing rate of the rabbit SAN cell in a use-dependent manner (Bois et al., 1996), and about 15% reduction of the pacemaking rate was observed at a concentration of 3 μM, which produced about 60% I_f reduction at membrane potential of −92 mV, and about 41% I_f reduction at physiologically relevant membrane potentials (∼60 mV) (Yaniv et al., 2012). Numerically, in a recent in silico exploration of the role of I_f in SAN pacemaking using a rabbit SAN model, the effect of ivabradine was simulated through implementing a 66% reduction of I_f (mimicking an experimentally reported effect of 3 μM ivabradine), leading to a 22% reduction in spontaneous rate (Severi et al., 2012). However, due to the non-linear concentration-dependent action of ivabradine on I_f, it is hard (if not impossible) to derive the effect of a low concentration of ivabradine from that of a high concentration on modulating cardiac pacemaking rate. To date, therefore, the effect of blocking I_f at the level of I_f reduction at clinical plasma levels of ivabradine (<20%) on pacemaking rate of the rabbit SAN has not been elucidated, as is how such concentration can produce a marked effect on the human SAN, in which I_f is much smaller than that in the rabbit SAN. Most importantly, it is unclear either how clinical concentrations of ivabradine affect cardiac pacemaking activity *in vivo* as compared to those predicted by single cell experiments *in vitro*, in which vagal tone modulation of cardiac pacemaking is missing. The aim of the present study was therefore to investigate through simulations and theoretical analysis the effect of I_f reduction over a wide range of values on cardiac pacemaking activity in the presence and absence of vagal tone modulation of cardiac pacemaking activity by acetylcholine.

METHODS

SAN Cell Model and I_f Formulations

In this study, the contemporary model of rabbit SAN cells developed by Severi et al. (2012) was used as a basal model. The model was chosen as it represents the most updated progress in the model development of rabbit SAN cells, in particular it incorporates an updated I_f formulation based on recently available experimental data (Altomare et al., 2003; Barbuti et al., 2007). The basal model code was downloadable from cellML at the following URL: https://models.physiomeproject.org/e/139; and the source codes used for this study are available on request to: henggui.zhang@manchester.ac.uk. In brief, the dynamics of the membrane action potential the SAN cell were modeled as:

$$\frac{dV}{dt} = -\frac{i_{total}}{C_m} \tag{1}$$

$$i_{total} = I_{CaL} + I_{CaT} + I_{Kr} + I_{Ks} + I_{sus} + I_{to} + I_{NaK} + I_{NaCa} + I_{Na} + I_f$$

Where V is the membrane potential, C_m the membrane capacitance, t the time, I_{total} the total membrane current generated by potassium (I_{Kr}, I_{Ks}, I_{sus}, I_{to}), calcium (I_{CaL}, I_{CaT}), sodium (I_{Na}), Na^+-K^+ pump (I_{NaK}), Na^+-Ca^{2+} exchanger (I_{NaCa}), and funny (I_f) channels. More details of the basal model are documented in the study of Severi et al. (2012).

Previous experimental studies have shown some distinctive differences in the maximal macroscopic conductance, the steady-state activation curve and the time constant of the channel activation of I_f between the rabbit and the human SAN cells (Difrancesco et al., 1989; Altomare et al., 2003; Barbuti et al., 2007; Verkerk et al., 2007b). In order to take into consideration the reported species difference in I_f properties, in our simulations we implemented two different sets of I_f formulations, one is the original model formulations developed by Severi et al. (2012) (rabbit-like formulation), and the other is Fabbri et al. formulation (Fabbri et al., 2017) based on the human I_f data (Verkerk et al., 2007b) (human-like formulation), which takes the form:

$$I_f = I_{f,Na} + I_{f,K}$$

$$I_{f,Na} = g_{f,Na} \cdot y \cdot (V - E_{Na})$$

$$I_{f,K} = g_{f,K} \cdot y \cdot (V - E_K)$$

$$\tau_y = \frac{1}{(0.36 \cdot (V + 148.8)/(e^{0.066 \cdot (V+148.8)} - 1) + 0.1 \cdot (V + 87.3)/(1 - e^{-0.21 \cdot (V+87.3)})} - 0.054$$

$$y_\infty = 0.01329 + 0.99921/(1 + e^{(V+97.134)/8.1752}), \quad \text{if } V < -80\text{mV}$$

$$y_\infty = 0.0002501 \cdot e^{(-V/12.861)}, \text{if } V \geq -80\text{mV}$$

$$\frac{dy}{dt} = \frac{y_\infty - y}{\tau_y}$$

where $I_{f,Na}$ and $I_{f,K}$ are Na^+ and K^+ components of I_f, $g_{f,Na}$ (0.00268 μS) and $g_{f,K}$ (0.00159 μS) conductance of $I_{f,Na}$ and $I_{f,K}$. E_{Na} and E_K the equilibrium potential for Na^+ and K^+. y_∞ is the steady state activation variable, τ_y the time constant of activation variable (y).

To determine and validate the parameters in the equations of human-like and rabbit-like I_f formulations, the equations for the steady-state activation curves (**Figure 1A**), and the equation for the activation time constant (**Figure 1B**) were fitted to experimental data obtained from human and rabbit SAN cells respectively (Difrancesco et al., 1989; Altomare et al., 2003; Barbuti et al., 2007; Verkerk et al., 2007b). The developed I_f formulations were validated by their ability to reproduce experimental I-V relationship data (**Figure 1C**) obtained by running a series of voltage-clamp commands (**Figure 1D**) for both the human-like and rabbit-like formulations. **Figure 1** shows clearly that I_f in the human SAN has a more negative half-maximal activation voltage (**Figure 1A**), a greater activation time constant (i.e., slower activation process (**Figure 1B**) and a smaller current density (**Figure 1C**) than that in the rabbit SAN.

Simulating the Effects of I_f Blockade

It has been shown that ivabradine blocks I_f without affecting channel kinetics, with block leading to a constant level of I_f reduction after a period of transition (Bucchi et al., 2002, 2013). Therefore, in this study, we implemented a pore-block theory (Yuan et al., 2015) to simulate the steady-state effect of I_f blocking by ivabradine over a wide concentration range by reducing its conductance by a factor k ($k \in$ (0,1), mimicking 0–100% (Bucchi et al., 2013) of I_f reduction. With varying levels of I_f inhibition, by the pore-block theory the I_f conductance became:

$$\begin{cases} g'_{fNa} = (1-k) \cdot g_{fNa} \\ g'_{fK} = (1-k) \cdot g_{fK} \end{cases}$$

Simulating the Effect of Acetylcholine (ACh)

In vivo, ACh released from vagal activity slows down the spontaneous pacing rate of the SAN mainly by inhibiting I_f and I_{CaL} (Boyett et al., 1995), and activating acetylcholine-dependent K^+ current (I_{KACh}) (Voigt et al., 2014). Vagal activity may also play a significant role in slowing down the pacing rate when ivabradine blocks I_f. To test the combined action of ivabradine and ACh, we simulated the ACh effect on SAN spontaneous APs, based on the formulations of Severi et al. (2012) for I_f and I_{CaL} inhibition, as well as I_{KACh} activation. In simulations, the values of $g_{K,ACh}$ used were the same as those used in the Severi et al. (2012) and Fabbri et al. models (Fabbri et al., 2017) for the human-like model (Severi model with human-like I_f) ((Fabbri et al., 2017) and the rabbit-like model (i.e., the Fabbri et al. model with rabbit-like I_f; see details in the **Supplementary Material**) (Severi et al., 2012). Effects of ACh on pacemaking APs were qualitatively analyzed and compared with the implementation of rabbit-like and human-like I_f formulation, as well as I_f blocking. Details of the I_{KACh} formulation were listed in the **Supplementary Material**.

Study of Model-Dependence

In order to test the model-dependence of results, simulations were also conducted in the Fabbri et al. model of the human SAN cell (Fabbri et al., 2017), the source code of which was downloadable from cellML at the following URL: https://models.physiomeproject.org/e/568?searchterm=human++si. In this case, the Fabbri et al. model with the human-like I_f formulation was taken as the basal model, which was then modified by replacing the I_f formulation by the rabbit-like one.

Although simulated action potentials from the original Fabbri et al. (2017) model closely match experiment data of AP properties and calcium transient of human SAN cells, some modification was necessary as most of the ionic currents in the model (except I_f, I_{Kr}, and I_{Ks}) were based on rabbit SAN cell model, densities of which were modified by automatic optimization to match simulated action potential characteristics to experimental data. Such automatic optimization of model parameters may deviate from physiological relevance, resulting in some limitations. For example, a full block of I_{CaT} in the model abolished the pacemaking action potential. Though there are no direct experimental data from human SAN cells to validate the simulation result, data from rabbit sinoatrial node (Hagiwara et al., 1988; Takeda et al., 2004) and human patients (Madle et al., 2001) suggested a more modest change in the pacemaking cycle length when I_{CaT} was blocked. Therefore, we updated the model to address some of the limitations. Details about model updating and validations are presented in **Supplementary Figure 1**. Using the updated model, simulations in the Serveri et al. model were repeated in the Fabbri et al. model, and results are included in the **Supplementary Material** to support the major conclusion of the study.

Numerical Scheme

A fourth-order Runge-Kutta-Merson numerical integration method was used to solve the ordinary differential equations of the model. The time step was 5×10^{-6} s, which gives a stable solution of the equations and maintains the accuracy of the computation of membrane current and potential. In simulations, action potentials after the 20th one were recorded for analysis. For solving the Severi et al. model with the human I_f formulation, a set of initial values were used, which were taken from the recorded state variables when the model reached its steady state (see details about the initial values for solving the model in the **Supplementary Material**). This allows the secondary effect of different I_f formulations to other channel variables of the models to be considered in the simulations.

Theoretical Analysis

Theoretical analysis of the effect of I_f block on altered cardiac pacemaking cycle length (CL) was conducted following a similar approach as implemented in previous studies (Rocchetti et al., 2000; Zaza and Lombardi, 2001; Monfredi et al., 2014; Winter and Shattock, 2016; Zaza, 2016).

Figure 2 shows a schematic illustration of a cycle of action potentials of SAN cells. During the time course of the action potential, the voltage difference between the MDP and the voltage at the beginning of AP upstroke (V_{up}) (ΔV_m) can

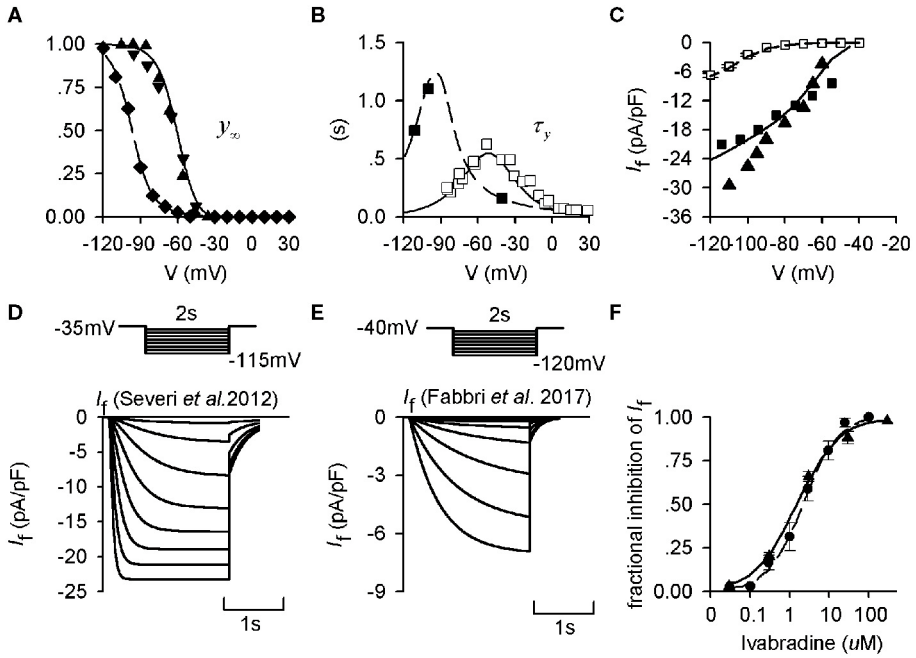

FIGURE 1 | Kinetics of I_f from experimental and mathematical modeling data. **(A)** Steady-state activation curves in rabbit and human and SAN cells, which were used to fit I_f formulations for the Severi et al. (2012) rabbit (solid lines) and the modified Fabbri et al. (2017) human (dashed lines) models. Experimental data from Altomare et al. (2003) (▲), Barbuti et al. (2007) (▼), and Verkerk et al. (2007b) (♦) are also shown. **(B)** Corresponding activation time constant of I_f for human and rabbit SAN cells. Experimental data from Difrancesco et al. (1989) (□) and Verkerk et al. (2007b) (■) are also shown. **(C)** Computed *I-V* relationship for the human- (dashed line) and rabbit-like (solid line) models, which are compared with experimental data from the study of Verkerk et al. (2007b) (□) for the human SAN cells, Zaza et al. (1996) (■) and Goethals et al. (1993) (▲) for the rabbit SAN cells. **(D,E)** Voltage-clamp protocol and simulated time traces of I_f during voltage-clamp for the rabbit and human I_f model. **(F)** Dose-dependent effect of ivabradine on I_f in rabbit SAN cells. Experimental data of Bois et al. (1996) (•) and Bucchi et al. (2002) (▲) were based to develop the concentration-response curves as shown by the solid line and dashed line respectively.

be discretized as many small steps by ΔV_i, each taking a time period DI_i to complete. Here dV_i/dt represents the local diastolic depolarization rate (DDR). During the diastolic depolarization phase, with small time interval (dt), $|dV_i/dt|$ can be approximately considered as a constant and denoted by $|dV/dt|$. And the total diastolic interval (DI) can be expressed as:

$$DI = \sum DI_i = \sum \frac{\Delta V_i}{|dV_i/dt|} = \frac{\sum \Delta V_i}{|dV/dt|} = \frac{\Delta V_m}{|dV/dt|} \quad (2)$$

Considering Equation (2), the pacemaking cycle length (CL) can be denoted as:

$$CL = APD + DI = APD + \frac{\Delta V_m}{|dV/dt|} = APD + \frac{C_m \Delta V_m}{|I_{total}|}$$

Where I_{total} denotes total membrane currents during the diastolic depolarization phase.

In response to I_f block, a new total ion channel current during the diastolic depolarization phase I'_{total} is generated, which takes the form

$$I'_{total} = I_{total} - \Delta I$$

ΔI is the change of I_{total} caused by I_f reduction. This produces a new pacing cycle length (CL′), which can be represented as:

$$CL' = APD' + \frac{C_m \Delta V_m}{|I'_{total}|} = APD + \frac{C_m \Delta V_m}{|I_{total} - \Delta I|}$$

where APD' is the new action potential duration in response to I_f blockade. As a small I_f block in response to a low dose of ivabradine mainly affects the diastolic depolarization phase and has little or no impact on the AP duration and the MDP, APD′ is approximately equal to APD. Therefore, the increased cycle length (ΔCL) can be represented as

$$\Delta CL = CL' - CL = C_m \Delta V_m \left(\frac{1}{|I_{total} - \Delta I|} - \frac{1}{|I_{total}|}\right)$$
$$= C_m \Delta V_m \frac{|\Delta I|}{|I_{total}| \cdot |I_{total} - \Delta I|}$$

Then the relative change of the pacing cycle length is:

$$\frac{\Delta CL}{CL} = \frac{C_m \Delta V_m}{\left(APD + \frac{C_m \Delta V_m}{|I_{total}|}\right)} \cdot \frac{1}{|I_{total}|} \cdot \frac{|\Delta I|}{|I_{total} - \Delta I|}$$

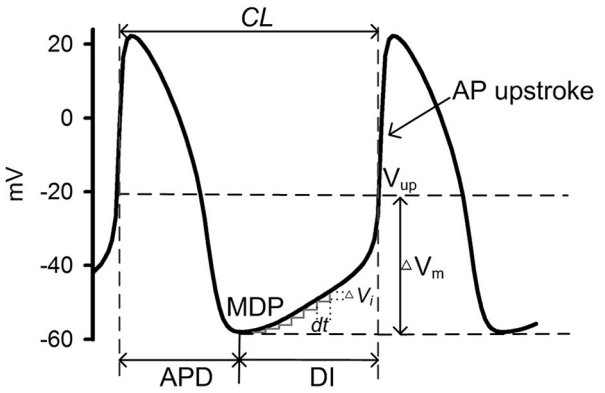

FIGURE 2 | Schematic illustration of a cycle of SAN cell action potentials. During one cycle, the time interval between two consecutive action potentials measures the intrinsic pacemaking CL, which can be considered as a sum of the AP duration (APD) and the diastolic interval (DI) which starts from the maximum diastolic potential (MDP) to the beginning of AP upstroke [V_{up} (Fabbri et al., 2017)]. ΔV_m denotes the voltage difference between the MPD and the V_{up}. During the DI, multiple time intervals (d*t*) were needed for the membrane potential to transit from the MDP to the V_{up}, during each of which a ΔV_i is generated.

By denoting p as I_f current block potency ($p = |\Delta I/I_f|$), and x as the proportion of I_f to I_{total} during the diastolic phase ($x = |I_f/I_{total}|$), then we have:

$$\frac{\Delta CL}{CL} = \frac{C_m \Delta V_m}{(APD + \frac{C_m \Delta V_m}{|I_{total}|})} \cdot \frac{1}{|I_{total}|} \cdot \frac{|\Delta I/I_f|}{|I_{total}/I_f - \Delta I/I_f|} = \frac{p}{(\frac{APD}{C_m \Delta V_m}|I_{total}| + 1)} \cdot \frac{1}{|\frac{1}{x} - p|}$$

By setting

$$C_1 = \frac{APD}{C_m \Delta V_m}$$

where C_1 ($C_1 > 0$) can be considered as a constant during the diastolic depolarization phase with a fixed level of I_f reduction (i.e., p is fixed), which has no significant effect on the difference between MDP and the V_{up} (i.e., ΔV_m), then we have:

$$\frac{\Delta CL}{CL} = \frac{p}{(C_1 |I_{total}| + 1)} \cdot \frac{1}{|\frac{1}{x} - p|} \propto C_2 \cdot \frac{1}{|I_{total}|} \cdot \frac{1}{|\frac{1}{x} - p|} \quad (3)$$

Where C_2 also can be seen as a constant related to C_1 and p, also with a fixed level of I_f reduction.

With I_f block, the resultant relative change of the CL predicted by Equation (3) is inversely proportional to the amplitude of I_{total} during the diastolic depolarization phase, which determines the intrinsic CL of the pacemaking action potential. It is also related to the level of I_f reduction and the ratio between I_f and I_{total}. With a small level of I_f block, the resultant relative change of CL is greater for a smaller I_{total} (i.e., greater when the CL is larger or the heart rate is lower).

RESULTS

Simulation Results

Figure 3 shows the simulated action potentials from the Severi et al. model with rabbit (**Figures 3Ai–Fi**) and human (**Figures 3Aii–Fii**) I_f formulations. In the figure, action potentials (**Figures 3Ai,Aii**) are shown together with membrane currents during the genesis of action potentials, including I_{CaL} (**Figures 3Bi,Bii**), I_f (**Figures 3Ci,Cii**), I_{Na} (**Figures 3Di,Dii**), I_{CaT} (**Figures 3Ei,Eii**), I_{NaCa} (**Figures 3Fi,Fii**), I_{Kr} (**Figures 3Gi,Gii**), I_{Ks} (**Figures 3Hi,Hii**), I_{to} (**Figures 3Ii,Iii**), and I_{NaK} (**Figures 3Ji,Jii**). By replacing the rabbit I_f formulation with the human I_f formulation, the pacemaking activity was slowed down, with a pacemaking CL that increased from 355 ms to 1,139 ms, which was associated with a slight increase in I_{Na} and I_{CaT} at the late period of the diastolic depolarization phase (DDP) (with no noticeable difference at the initial period of the DDP), and a slight decrease in I_{Kr}, I_{Ks}, I_{to}, and I_{NaK} during the DDP. Such a small increase in the above-mentioned inward currents and a decrease in the outward currents, though contributory factors, are not the major determinants of the prolonged diastolic depolarization phase. The slowing down in the pacemaking activity of the human-like formulation model is mainly attributable to the smaller I_f, I_{CaL}, and I_{NaCa} during the diastolic depolarization phase.

In **Figure 3**, effects of reducing I_f by 20% on the pacemaking activity of the two models are also shown.

Reduction of I_f by 20% produced an increase of the CL in the rabbit-like I_f formulation model by about 4.6% (**Figure 3K**). This is in agreement with experimental data from isolated rabbit SAN cells, which showed that a low level of I_f block by ivabradine [$<0.5\,\mu M$, a concentration not affecting SAN I_{CaL} which only slightly decreased by $18.12 \pm 0.66\%$ at $10\,\mu M$ (Bois et al., 1996)] produced only a slight slowing down of the pacemaking rate, while $>50\%$ I_f blockade by $3\,\mu M$ ivabradine (see **Figure 1F**) only reduced the spontaneous pacing rate by 11–17.7% (Bucchi et al., 2007; Yaniv et al., 2012).

However, in the human-like I_f formulation model, I_f reduction by 20% produced a more than 2-fold increase in the pacemaking CL by 12.4% (i.e., equivalent to about 11.1% reduction in the heart rate) as compared to the rabbit-like model (**Figure 3K**). The pacing rate reduction though was slightly less than the effect of intravenous administration of ivabradine by 0.2 $mg{\cdot}kg^{-1}$ (∼23.5–34.1 nM of mean maximal ivabradine plasma levels) produced a reduction of heart rate by 18–20% (i.e., mean heart rate reductions of 12.9 and 14.1 beats min^{-1}; Camm and Lau, 2003; Jiang et al., 2013), but close to experimental data of the pacing rate reduction when I_f was blocked by $3\,\mu M$ ivabradine in rabbit SAN (Bucchi et al., 2007; Yaniv et al., 2012). This illustrates that the small human-like I_f has a greater effect on slowing down the pacing rate than the rabbit-like one when I_f is inhibited by ivabradine.

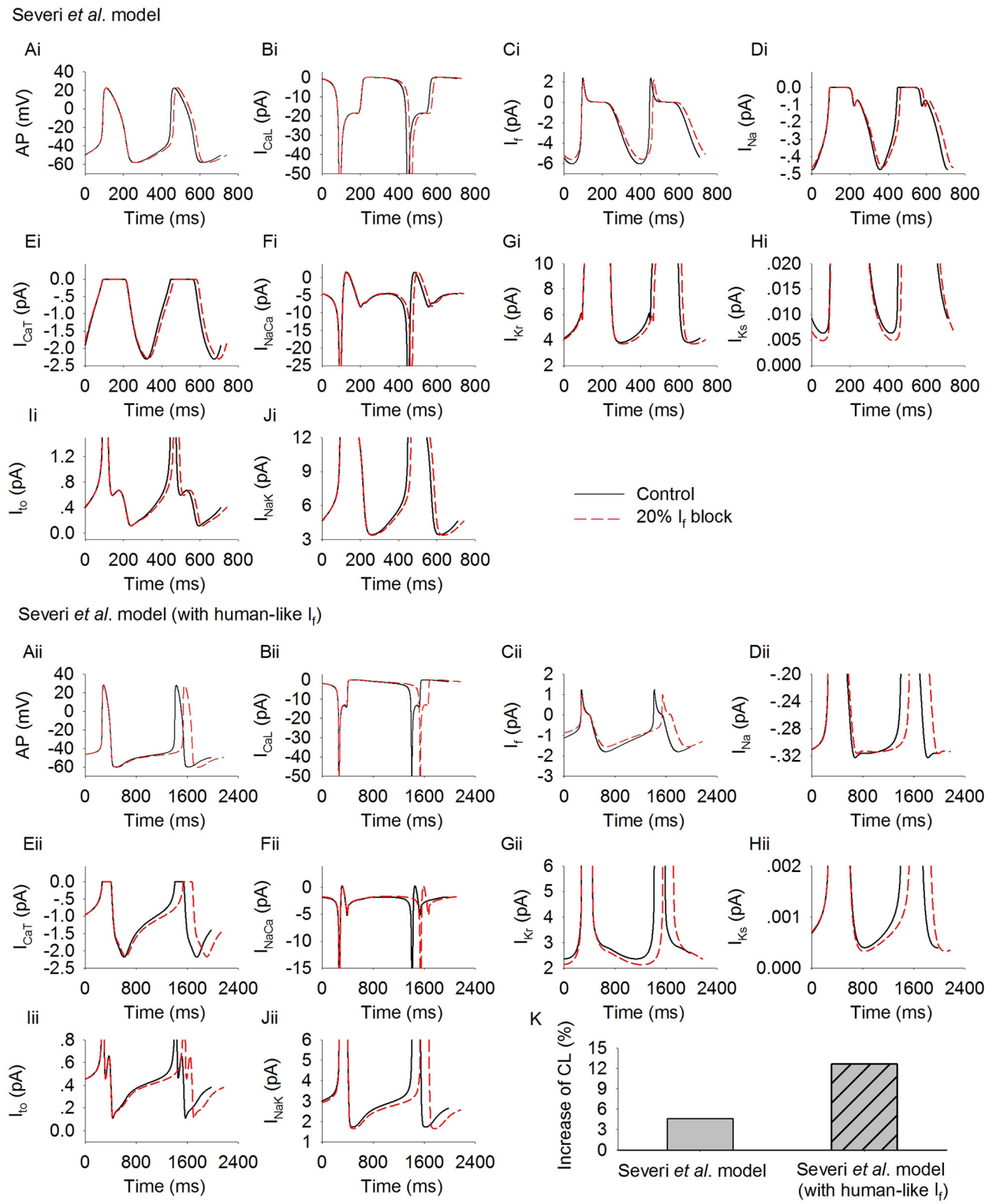

FIGURE 3 | Simulated spontaneous action potentials and underlying currents by the Severi et al. model with rabbit I_f **(Ai–Fi)** and human I_f **(Aii–Fii)** formulations. Effects of blocking I_f by 20% on action potentials and underlying ionic currents (dotted lines) are also shown and superimposed with those in control condition (solid lines). **(Ai,Aii)**: action potentials; **(Bi,Bii)**: I_{CaL}; **(Ci,Cii)**: I_f; **(Di,Dii)**: I_{Na}; **(Ei,Eii)**: I_{CaT}; **(Fi,Fii)**: I_{NaCa}; **(Gi,Gii)**: I_{Kr}; **(Hi,Hii)**: I_{Ks}; **(Ii,Iii)**: I_{to}; **(K)** increase of pacing CL.

The results above suggested that the increased CL induced by 20% I_f reduction is proportional to the intrinsic cycle length of the model, i.e., the greater the intrinsic CL (e.g., the model with human-like I_f formulation) the greater the increase of the CL. This observation was model-independent as shown in **Supplementary Figure 3**, in which Fabbri et al. model of the human SAN was implemented by using rabbit-like and human-like I_f formulations. In the basal condition (Fabbri et al. model with human-like I_f formulation), the CL was 810 ms, which was increased by 44 ms with 20% I_f reduction (i.e., 5.5%). When the rabbit-like I_f formulation was used, the pacemaking rate was increased due to a larger I_f, resulting a CL of 355 ms. With 20% I_f reduction, the CL was increased by 18 ms (i.e., 4.7%), which was smaller than that when the human-like I_f formulation was used.

As shown in **Figures 3Ci,Cii**, a 20% reduction in the channel conductance did not necessarily produce 20% reduction in I_f amplitude during the time course of action potential, due to the dependence of I_f on membrane voltage. To further investigate this, we computed the average I_f during the diastolic phase before and after 20% reduction in its channel conductance. Results are shown in **Supplementary Figure 2**. It was found that 20% reduction in the channel conductance produced a similar decrease in the avarage I_f in the rabbit-like (by 0.34 pA) and the human-like model (by 0.22 pA), but the relative change was greater in the latter model because of its smaller I_f in the control condition. Such difference in the relative change of I_f may also be one of the important reasons for the more pronounced prolongation of the diastolic phase in model with human I_f formulation. Note that in both models (rabbit-like and human-like models), the relative change of I_f was smaller than 20% though the channel conductance was reduced by 20%, due to the voltage-dependence of the channel's activation.

Further simulations were carried out to analyze possible effects of the cross talk between the membrane clock (I_f) and Ca^{2+} clock on modulating pacemaking action potentials in response to I_f reduction. **Figure 4** shows results for the rabbit-like (**Figures 4Ai–Ei**) and human-like (**Figures 4Aii–Eii**) I_f formulation models. Blocking I_f by 20% decreased intracellular (cytoplasmic) Ca^{2+} transients ($[Ca^{2+}]_i$, **Figures 4Bi,Bii**), the intracellular subspace Ca^{2+} concentration ($[Ca^{2+}]_{sub}$, **Figures 4Ci,Cii**) and the Ca^{2+} content in the network SR ($[Ca^{2+}]_{nsr}$, **Figures 4Ei,Eii**). The diastolic level of $[Ca^{2+}]_{sub}$ was reduced by 2.9 and 5% in the rabbit-like and human-like I_f formulation model respectively, the decreased $[Ca]_{sub}$ during the diastolic depolarization phase of the action potential (**Figures 4Ci,Cii**) leads to a decreased I_{NaCa} (**Figures 3Fi,Fii**) and I_{CaL} (**Figures 3Bi,Bii**), especially during the later phase of diastolic depolarization, which prolonged the later phase of the diastolic depolarization in the human-like I_f formulation model (**Figure 4Aii**). There was a negligible change in I_{Na} (**Figures 3Di,Dii**) and I_{CaT} (**Figures 3Ei,Eii**) during the diastolic phase. Taken together with the observation of changes in I_{NaCa} (**Figure 3F**), our simulation results imply that the slowing down of the spontaneous action potentials in response to a low level of I_f block (< 20%) may be mainly attributable to I_f reduction (i.e., membrane clock), with some contribution from a crosstalk between the membrane clock and Ca^{2+} clock in the later diastolic depolarization phase.

Effects were also investigated of how a systematic change in I_f density affects spontaneous pacemaker activity. Results are shown in **Figure 5**, in which the computed CL (**Figure 5A**) and its increase (**Figure 5B**) with I_f being blocked from 0 to 100% with 1% increment for the rabbit-like (closed circles) and human-like I_f formulations (open circles). It was shown that over the range 0–80%, I_f block produced a greater CL increase with the human-like formulation than in the rabbit-like model. With a low level of I_f reduction, a linear relationship between the CL increase and I_f block was seen (**Figure 5B**). However, the relationship changed to an exponential one (**Figure 5B**) when a high level of I_f block was implemented. With about 66% I_f reduction, the CL was increased by about 26% (reduced pacemaking rate by 21%) in the rabbit-like model, which is consistent with experimental data (Thollon et al., 1994; Bucchi et al., 2007), but by about 42% in the human I_f formulation. A low level of I_f reduction (<20%) resulted in a negligible change in the MDP (<-0.3 mV in both models) in both rabbit-like and human-like I_f formulation models, and 100% I_f reduction hyperpolarised MDP by only 3.2 mV in the latter model (**Figure 5C**). Corresponding changes in APD_{90} (**Figure 5D**) and the voltage at the beginning of AP upstroke (**Figure 5E**) were also shown (also see **Supplementary Table 1**). While a high level of I_f reduction hyperpolarized the MDP, it had modest secondary effect on APD_{90} (mainly prolonging the late repolarization phase which may be due to the decreased I_{Kr} and I_{NaK} as shown in **Supplementary Figures 4Gi,Ji**, and there was no significant change in the fundamental morphology of the action potential as shown in **Supplementary Figure 4Ai**) and AP upstroke potential in the rabbit-like model.

Changes of the membrane currents and ion concentrations with a systematic change in I_f density in the two models were also investigated (**Supplementary Figures 3, 4**). During the diastolic depolarization phase of the action potentials, $[Ca]_{sub}$ decreased as I_f density gradually decreased (**Supplementary Figures 3Ci,Cii**), further leading to a slower activation of the I_{CaL} (**Supplementary Figures 4Bi,Bii**) and a decrease in I_{NaCa} (**Supplementary Figures 4Fi,Fii**) during this phase. Reduction *of* I_{NaCa} decreased $[Na]_i$ (**Supplementary Figures 3Fi,Fii**), leading to a reduction in I_{NaK} (**Supplementary Figures 4Ji,Jii**) which further exacerbated the reduction of $[Na]_i$. The outward currents (I_{Kr}, I_{Ks}, I_{to}, I_{NaK}) also showed a gradual decrease with a decreased I_f density during the diastolic depolarization phase (**Supplementary Figures 4Gi–Ji,Gii–Jii**).

The simulated action potentials from the two models showed some differences when I_f was fully blocked (**Figure 5A**), with the rabbit-like model failing to generate spontaneous action potentials. Such differences may be attributable to the use of different sets of initial values recorded from their steady state variables as there was no other changes in model equations or parameters, except for the use of rabbit-like I_f or human-like I_f formulations. In order to determine potential

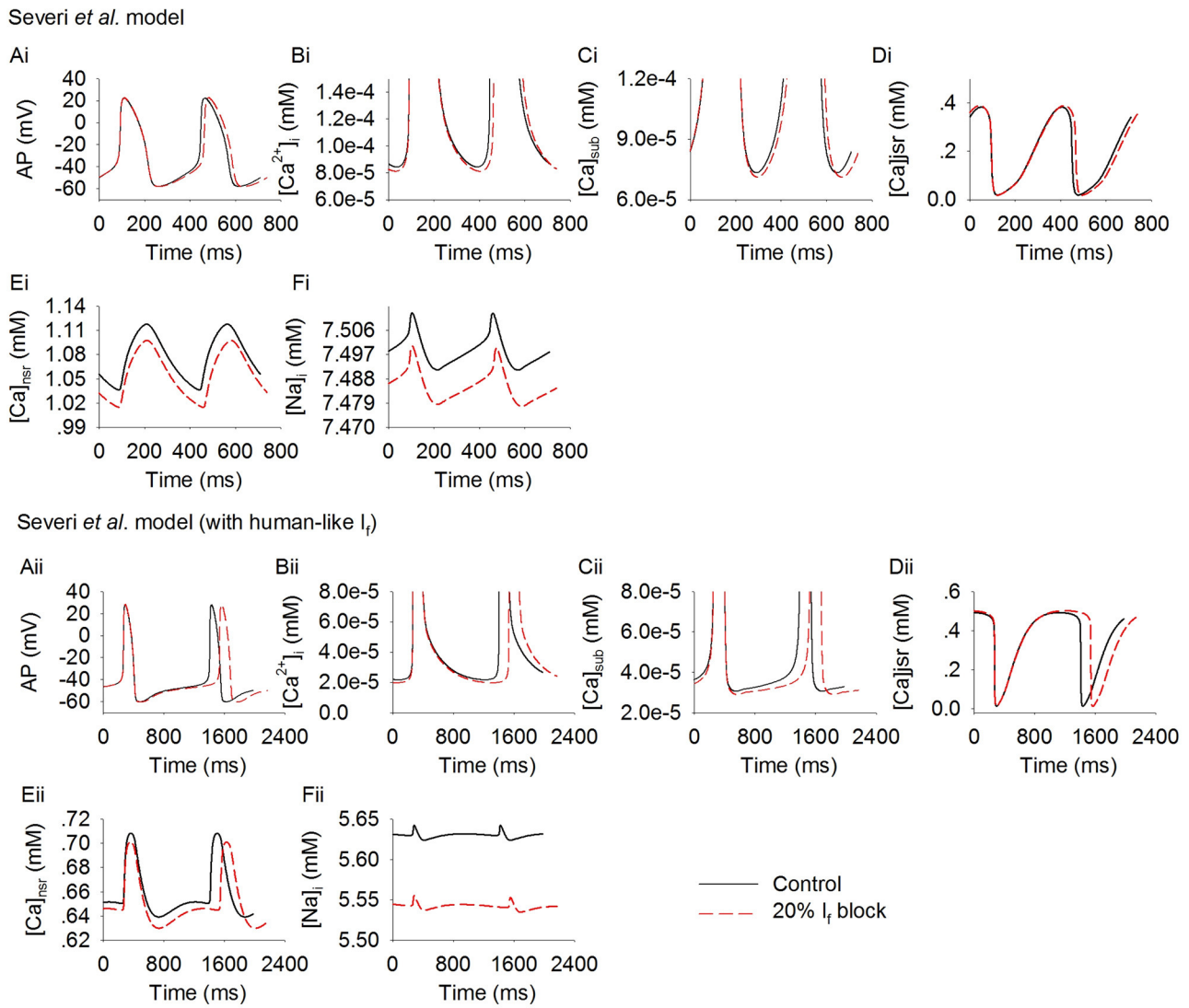

FIGURE 4 | Effect of I_f block on the Ca^{2+} transient in rabbit-like **(Ai–Ei)** and human-like **(Aii–Eii)** SAN cell models. **(Ai,Aii)**: the action potentials; **(Bi,Bii)**: Ca^{2+} transient in the myoplasmic space; **(Ci,Cii)**: Ca^{2+} transient in the myoplasmic sub-space; **(Di,Dii)**: Ca^{2+} transients in the junctional SR; **(Ei,Eii)**: Ca^{2+} transient in the network SR space; **(Fi,Fii)**: intracellular Na^+ concentration. Simulation results in control (solid line) are superimposed on those of I_f blocking (dotted lines).

factors contributing to such differences or contributing to the pacemaking action potentials in the two models, further analyses on membrane currents and the intracellular Ca^{2+} transients between control and 99% reduction of I_f were conducted. Results are shown in **Supplementary Figures 3, 4**. It was shown that in both models, in addition to I_f, I_{CaT}, I_{NaCa}, and I_{Na} contributed to the diastolic depolarization. With a high level of I_f reduction (99%), there was a significant decrease in $[Ca]_{sub}$ during the diastolic depolarization phase (**Supplementary Figure 3Ci**), causing a significant reduction in I_{NaCa} (**Supplementary Figure 4Fi**). Consequently, the spontaneous membrane depolarization was not able to reach the I_{CaL} activation potential, terminating the action potentials in the rabbit-like model.

In the human-like model, a reduction of $[Ca]_{sub}$ was also observed with a high level of I_f reduction, resulting in a decreased I_{NaCa}. However I_{NaCa} was sufficient to maintain the spontaneous depolarization to generate a full action potential.

The focus of this study was on the action of a modest extent (i.e., <20%) of I_f bock, mimicking the clinical use of ivabradine, rather than on the action of a large percentage of I_f block. With <50% I_f block, the increase in CL was about <30%, which is reasonably close to the experimental data observed in rabbit SAN cells when I_f is blocked by use of Cs^+ (Nikmaram et al., 1997), validating the physiological relevance of the results obtained.

Further simulations were conducted to investigate the combined action of I_f reduction by ivabradine and actions of ACh (Boyett et al., 1995), mimicking the autonomic regulation

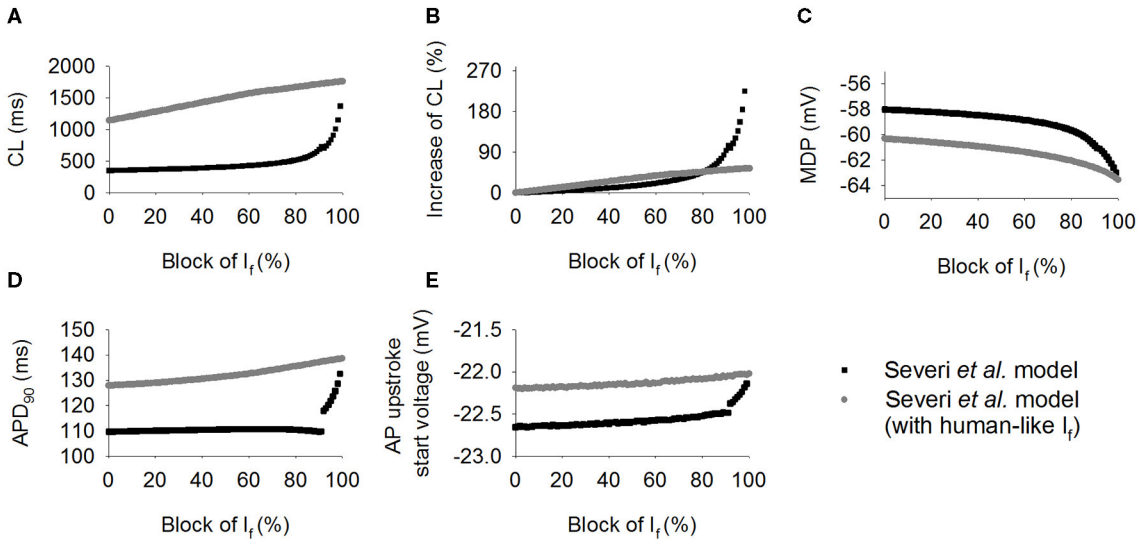

FIGURE 5 | Simulated effect of I_f block on the CL increase. **(A,B)** Pacing cycle length and the relative percentage changes of CL when I_f blocked from 0 to 100% with 1% increment in the human-like (open circle) and rabbit-like (closed circle) SAN cell models; **(C,D)** the maximum diastolic potential (MDP) and action potential duration at 90% of repolarization (APD_{90}); **(E)** change of the beginning of action potential upstroke voltage, which was calculated as the diastolic depolarization rate reached about 50% of its maximum value. I_f block produced greater effect in the human-like (gray circle) and rabbit-like (black square) SAN cell models.

of cardiac pacemaking *in vivo*. In simulations, acetylcholine-dependent inhibition of I_f and I_{CaL}, and activation of K^+ current ($I_{K,ACh}$) (Voigt et al., 2014) were considered. Results are shown in **Figure 6**, in which computed time courses of APs in control (with both rabbit-like and human-like I_f formulations), I_f reduction alone (by 20%) and I_f reduction together with actions of 0.1 nM ACh were compared (**Figures 6A,B**). It was shown that ACh augmented the effect of I_f reduction on the increase of CL in the model with both the rabbit-like and human-like I_f formulations. With the action of 0.1 nM ACh, 20% of I_f block increased the CL by 37.5% (about 27.3% reduction the pacing rate) (**Figure 6C**) in the model with human-like I_f formulation, which is remarkably greater than that of 10.1% (about 9.1% reduction in the pacing rat) in the model with the rabbit-like I_f formulation. This observation held true when different ACh concentrations were considered (**Figure 6D**). These results illustrate that the combined action of I_{KACh} and I_f reduction further slowed down the pacemaking AP due to a reduced total depolarization current during diastolic depolarization phase, resulting in a greater CL prolongation. It suggested that the clinical observed effect of low ivabradine on reducing pacing rate may partially result from the action of ACh due to active vagal tone *in vivo*. Similar observations were also seen in the Fabbri et al. model as shown in **Supplementary Figure 4**, in which ACh augmented more the effect of I_f reduction on pacemaking rate in the model with human-like I_f formulation than that with rabbit-like I_f formulation. Results from the Fabbri et al. model were similar, as shown in **Supplementary Figure 5**.

Theoretical Analysis Validation

The simulation results presented above showed that I_f block produced a greater impact on slowing down the pacemaking rate with the human-like I_f formulation than that in the rabbit-like cell model in both the Severi et al. and Fabbri et al. model (see **Supplementary Material**). This is paradoxical as the I_f density over the pacemaker range with the human-like formulation is much smaller than that in the rabbit-like model, and one would expect a smaller I_f contribution to the spontaneous action potentials (therefore a smaller CL increase with I_f block). However, such a paradoxical effect of I_f reduction on the increase of CL as observed in the two models matched the theoretical prediction shown in the Method section (Equation 2), which showed an inverse relationship between an increased CL and the amplitude of total ionic membrane currents during the diastolic depolarization phase. With the theoretical prediction, a greater CL increase in the human-like I_f formulation SAN cell model can be attributed to a smaller I_{total} during the diastolic depolarization phase.

To test the theoretical prediction, further analyses were conducted to compute the averaged I_{total} amplitude during the DDP. Results from the Severi et al. model are shown in **Figure 7** for control and 20% I_f reduction for action potentials (**Figures 7Ai,Aii**), the time course of I_{total} (**Figures 7Bi,Bii**) and the averaged amplitude of I_{total} (**Figure 7C**) during the DDP. It was found that during the time course of diastolic depolarization, the averaged I_{total} amplitude in the cell model with the human I_f formulations was much smaller (<30%) than that in the rabbit-like model, which produced a slower pacemaking rate (i.e., longer CL) and greater CL increase in response to 20% I_f reduction, matching the theoretical prediction. The changes in currents and Ca^{2+} ion concentration associated with the change in I_{total} (**Figures 7Bi,Bii**) are shown in **Figures 3**, **4**. A similar

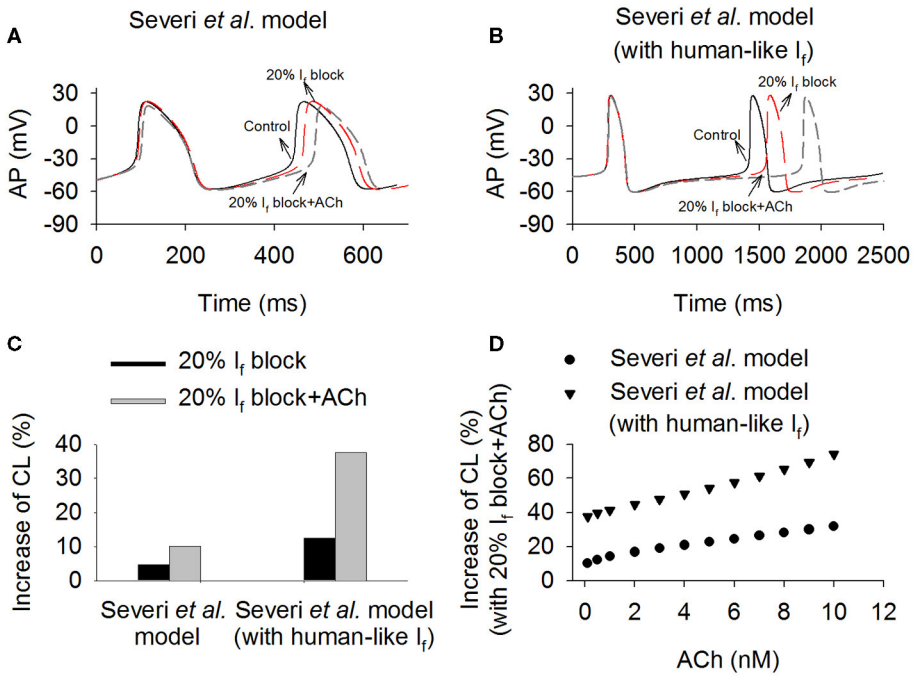

FIGURE 6 | Effects of combined action of ACh and 20% I_f reduction on sponteneous action potentials in the Severi et al. model with the rabbit-like and human-like I_f formulations. **(A,B)** Time courses of action potentials in control, I_f reduction and combined effect of I_f reduction and ACh (0.1 nM). **(C)** The increase of pacemaking CL in the conditions of 20% I_f block alone and combined action with ACh (0.1 nM). **(D)** Combined effect of variant concentrations of ACh (from 0.1 to 10 nM) and 20% I_f block on pacemaking CL in the rabbit-like and human-like I_f formulations models.

observation was also seen in the Fabbri et al. model as shown in **Supplementary Figure 6C**.

In theoretical analysis it was shown that the relative increase of CL was also influenced by a factor of $\frac{1}{|1/x-p|}$, which was related to the ratio of I_f to I_{total} (x) and I_f block potency (p). In simulations, we further computed the values of $\frac{1}{|1/x-p|}$ and $\frac{1}{|I_{total}|} \cdot \frac{1}{|1/x-p|}$ for control and I_f reduction cases. Results from the Severi et al. model are shown in **Figure 8**, in which the time courses of $\frac{1}{|1/x-0.2|}$ (**Figures 8Ai,Aii**) and $\frac{1}{|I_{total}|} \cdot \frac{1}{|1/x-0.2|}$ (**Figures 8Bi,Bii**) were plotted for the control (black) and 20% I_f reduction ($p = 0.2$) for the rabbit-like (left panels) and human-like (the right panels) models. The computed $\frac{1}{|1/x-0.2|}$ (acting as a piecewise function) was set to $\frac{1}{1\times10^{-3}}$ when $|1/x - 0.2|$ was smaller than 1×10^{-3} to avoid the value close to positive infinity. It was shown that in both models with a small I_f block the difference in the computed value of $\frac{1}{|1/x-p|}$ between control (solid line) and 20% I_f reduction (dotted line) was very small during diastolic depolarization phase, and also small when the value was normalized against I_{total} ($\frac{1}{|I_{total}|} \cdot \frac{1}{|1/x-0.2|}$). This provides support for the notion that the relative increase of CL was mainly determined by the amplitude of I_{total} during the diastolic depolarisation phase in response to I_f block.

Note that during the last period of diastolic depolarisation phase (i.e., during time period of 310–387 ms as shown in the figure for the rabbit-like model and 890–1,331 ms for the human-like model), the difference in the computed values of $\frac{1}{|1/x-0.2|}$ and $\frac{1}{|I_{total}|} \cdot \frac{1}{|1/x-0.2|}$ became more noticeable. This may be attributable to the different timings by which the upstroke of pacemaking actions potentials occurred between control and I_f reduction conditions. Note that the value of $\frac{1}{|1/x-0.2|}$ was also greater in the human-like model than that in the rabbit, which amplified the contribution of $\frac{1}{|I_{total}|}$ toward a relative increase of CL. Results from the Fabbri et al. model were similar, as shown in **Supplementary Figure 7**.

A marked difference in the $V_{1/2}$ of the steady-state activation relationship (y_∞) of I_f between the rabbit and the human SAN cells has been observed (Difrancesco et al., 1989; Altomare et al., 2003; Barbuti et al., 2007; Verkerk et al., 2007b). In this study, we used $V_{1/2}$ of −52.5 and −97.1 mV for the rabbit-like and the human-like I_f formulation respectively. In order to systematically determine a possible role of varying $V_{1/2}$ in modulating I_f amplitude, and thus the I_{total} and the effect of I_f reduction on the increase of CL, we changed $V_{1/2}$ of y_∞ in the human-like I_f formulation in a border range from −50 to−70 mV. Results from the Serveri et al. model are shown in **Figure 9** for the pacemaking CL (**Figure 9A**), the averaged I_{total} during diastolic depolarization phase (**Figure 8B**), and increase of CL (**Figure 9C**) with 20% I_f block. Shifting the $V_{1/2}$ from−50 mV (about rabbit $V_{1/2}$) to −70 mV (about human $V_{1/2}$), the I_{total} was decreased (**Figure 9B**), which were correlated with an increased CL (**Figure 9A**) as well as an increased effect of I_f reduction on CL (**Figure 9C**). These results supported our theoretical analysis on that a smaller I_f in the model resulted in a smaller I_{total}

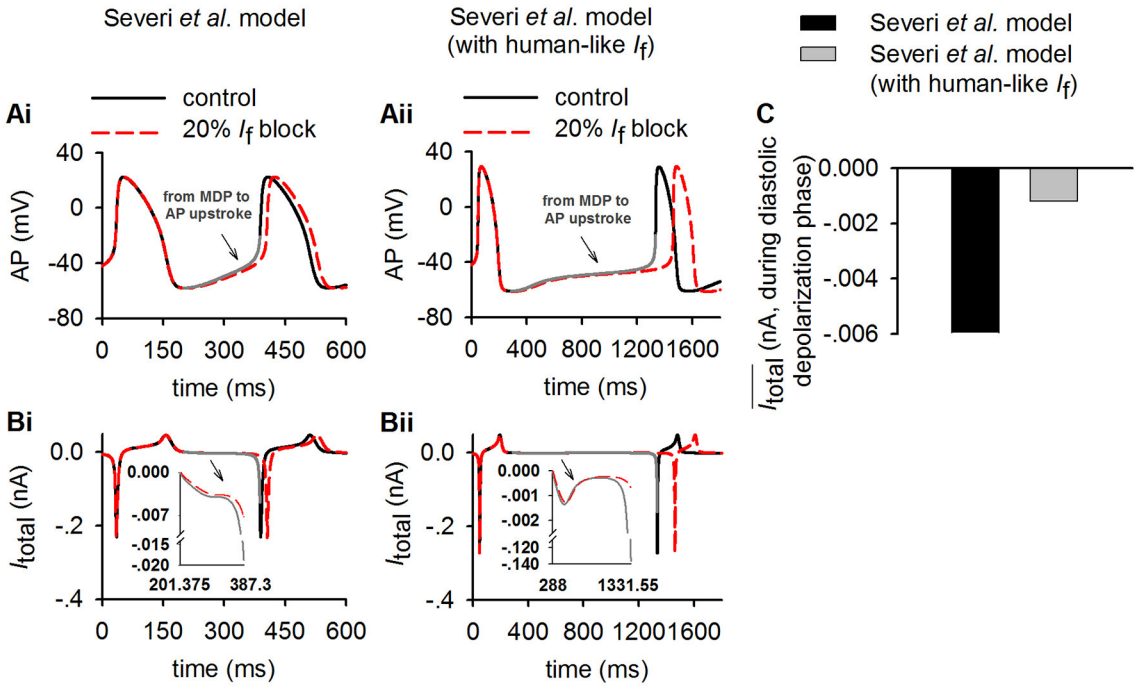

FIGURE 7 | Simulation of the inverse relationship of I_{total} and the increasing of CL in control (solid lines) and 20% I_f reduction (dotted lines) to validate theoretical analysis result (Equation 2) in method section ($p = 0.2$, modeling 20% I_f reduction). **(Ai,Aii)** Time course of action potentials for rabbit-like and human-like SAN cell models respectively (gray lines represents diastolic depolarization voltage changes from the MDP to the voltage at the beginning of AP upstroke in control condition); **(Bi,Bii)** time courses of I_{total} (gray lines represents diastolic depolarization voltage changes from the MDP to the voltage at the beginning of AP upstroke in control condition). **(C)** Averaged value of I_{total} amplitude during the diastolic depolarization phase for the rabbit-like (black) and human-like (gray) SAN cell models. In each case, the integral interval was set to the time interval between the MDP and beginning of the upstroke membrane potential (V_{up}).

amplitude, resulting in a slower pacemaking rate; and as such the same reduction in I_f resulted in a more significant change of CL in the cell model with a smaller I_{total}. Similar results were also observed using the Fabbri et al. model as shown in **Supplementary Figure 8**.

DISCUSSION

This study was conducted to determine the mechanism by which a low level of I_f block by clinical drug (ivabradine) concentration is able to reduce the heart rate of patients by about 18–20%. In a previous study, Verkerk and Wilders found that though I_f has a small magnitude in the human SA node cells, it has an equally important role as in the rabbit (Verkerk and Wilders, 2010). In another study, Maltsev and Lakatta argued that I_f provides a relatively modest contribution to spontaneous beating rate regulation of human and rabbit sinoatrial node cells, and its major role in human SAN cells is to prevent excessive hyperpolarization during AP repolarization, thus representing an anti-bradycardic mechanism, rather than a primary rate regulatory mechanism (Maltsev and Lakatta, 2010). Though these previous studies addressed how a smaller I_f can produce the same effect in humans with respect to rabbit (Verkerk and Wilders, 2010; Fabbri et al., 2017) on complete I_f block, however, the question on how <20% I_f block produces a marked heart rate reduction in humans in *vivo* had remained unclear. This is due to the nonlinear relationship between the extent of I_f block and heart rate reduction (see **Figure 5**); effects of partial I_f block cannot be predicted with certainty from the complete block data already in the literature.

The principal contributions of the work are insights into how a small extent of I_f block (<20%; as may occur during clinical use of ivabradine) produces a marked heart rate reduction in human SAN, greater than that predicted by single cell experiments in the rabbit though the latter has a greater I_f density. Our principal findings are: (i) blocking I_f by 20% resulted in only about a 4.6 % increase in the CL in the rabbit-like SAN cell model, but about 12.4% in the cell model with human I_f formulation. This finding suggests that I_f block has a greater effect with the human-like SAN cell I_f formulation than with rabbit-like I_f formulation, despite the fact that the former has a smaller I_f current density over diastolic potentials, based on which one might expect a smaller contribution of I_f to pacemaking; (ii) there is a cross-talk between the membrane clock and Ca^{2+} clock with 20% I_f block in the later phase of the diastolic depolarization of the action potential; (iii) a theoretical analysis matching the simulation data has been produced, providing a numerical formalism explaining the relationship between I_f block effects and its contribution to total current during diastolic phase. In this study, both numerical simulations and theoretical analysis here have attributed the paradoxical effect of I_f reduction (i.e., a greater effect in SAN cells with smaller I_f current density

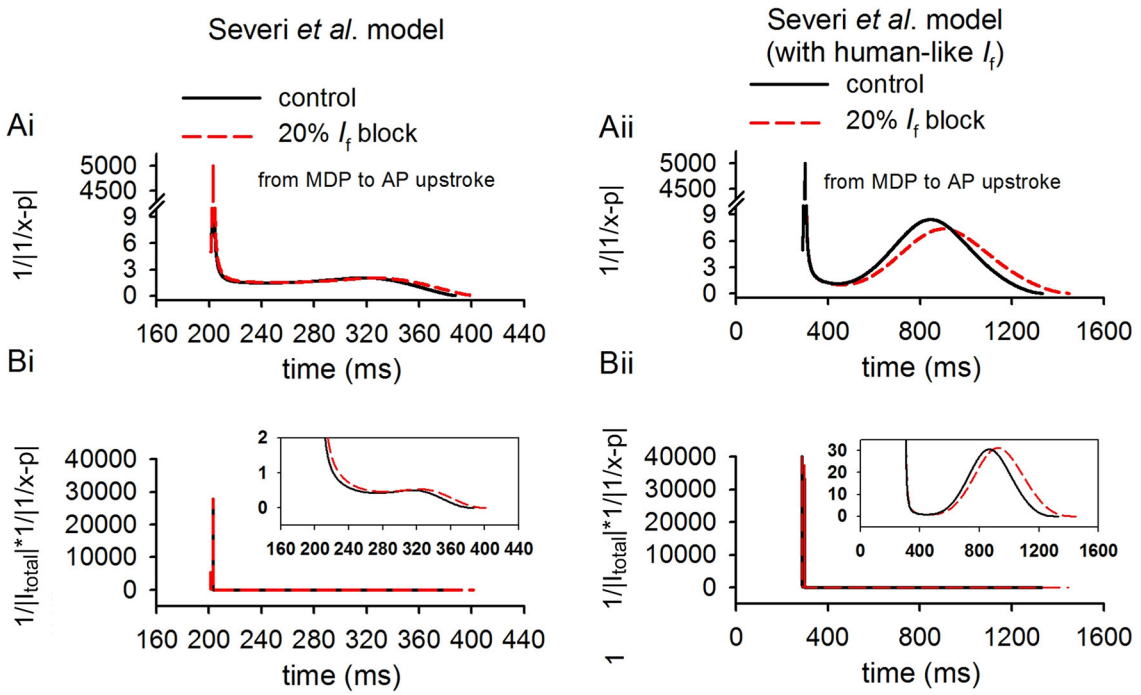

FIGURE 8 | Computed values of $\frac{1}{|1/x-p|}$ and $\frac{1}{|I_{total}|} \cdot \frac{1}{|1/x-p|}$ to validate theoretical analysis result (Equation 2) in method section ($p = 0.2$, modeling 20% I_f reduction). The highlighted lines shown in this figure are during the diastolic depolarization phase of the action potentials of control (solid lines) and 20% I_f reduction (dotted lines) cases for the rabbit-like **(Ai,Bi)** and human-like **(Aii,Bii)** SAN cell models.

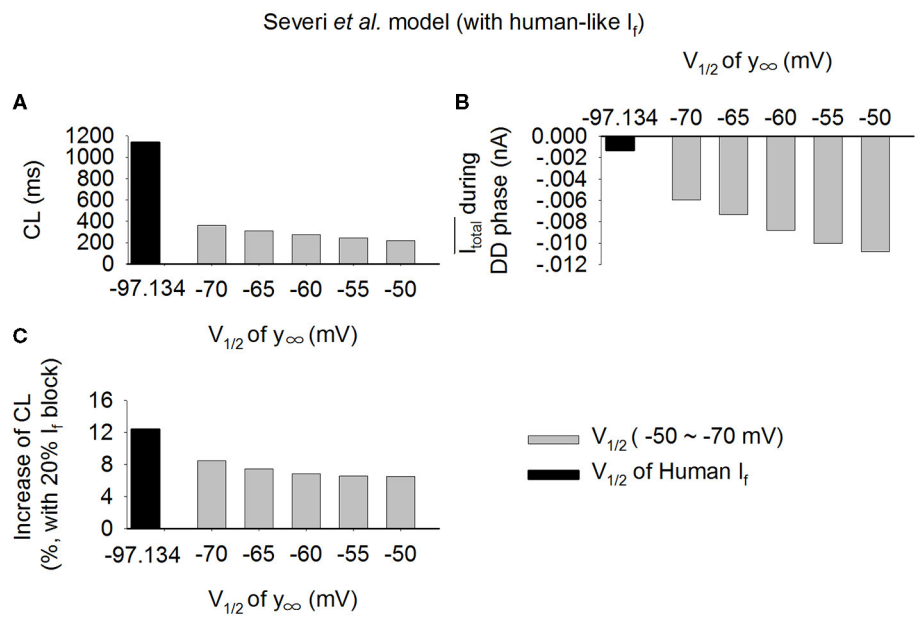

FIGURE 9 | (A–C) Effect of varied half-activation voltage ($V_{1/2}$) of the steady state activation variable (y_∞) on pacemaking CL in the Serveri et al. model with human-like I_f formulation. $V_{1/2}$ changed from −50 to −70 mV, covering the experimental data range for rabbit (−50 mV) and human (−97.1 mV) SAN cells.

and therefore a slower heart rate) to an inverse relationship between the relative increase of CL and the amplitude of the total current during the diastolic depolarization phase in response to I_f block; and (iv) significantly, vagal tone activity *via* ACh augments the effects of ivabradine on heart rate reduction, providing a possible mechanism(s) by which the clinical concentrations can

have larger effects *in vivo* than those predicted by single cell experiments *in vitro*. It has been shown that combined action of ACh (0.1 nM) and 20% I_f reduction markedly increase the pacemaking CL by 37.5%, close to the clinical effect of ivabradine when human-like I_f formulation was used, which is significantly greater than that of 10.1% when the rabbit-like I_f formulation was used. These findings were also observed in the Fabbri et al. model.

The results of the present study demonstrate and explain why a smaller human I_f has a greater effect on prolonging the diastolic depolarization phase when it is partially blocked, using both mathematical theoretical analysis and computer simulation, which is clearly distinct from the previous studies (Verkerk and Wilders, 2010; Fabbri et al., 2017). Collectively, they add mechanistic insight into the understanding of how a low dose of clinical use of ivabradine (<137 nM) can effectively slow down the human heart rate by about 18–20% (Camm and Lau, 2003; Joannides et al., 2006; Doesch et al., 2007; Jiang et al., 2013), which contrasts with a negligible effect predicted by experimental studies in the rabbit (<4% at 10 min after administration of ivabradine; Thollon et al., 2007).

Role of I_f in Generating Cardiac Pacemaking Activity

I_f channels encoded by HCN genes are richly expressed in cardiac conduction systems including the primary pacemaker, the SAN (Altomare et al., 2003; Ravagli et al., 2016). Previous studies from animal models have suggested an important role of I_f in the SAN (Difrancesco and Noble, 2012; Baruscotti et al., 2016; Kozasa et al., 2018). It has been shown that a complete block of I_f by Cs^+ (2 mM) slowed down the pacemaking rate by 30% in the rabbit SAN cells (Denyer and Brown, 1990), a 17.6% reduction of pacemaking rate also seen when blocking of I_f with 0.5 mmol/L Cs^+ (Liu et al., 2008). In transgenic mice, knocking down HCN4 produced bradycardiac effects as well as atrioventricular node conduction block (Herrmann et al., 2007; Hoesl et al., 2008; Baruscotti et al., 2011). All of this evidence demonstrates that I_f, together with the more recently identified Ca^{2+} clock [arising from the coupling between the intracellular Ca^{2+} cycling and electrogenesis of membrane currents (e.g., I_{NaCa}) (Maltsev and Lakatta, 2008; Lakatta and Difrancesco, 2009)], provide a major driving force for generating the spontaneous depolarization during the diastolic phase that leads to intrinsic pacemaker activity.

I_f is also present in human SAN cells (Verkerk et al., 2009b; Li et al., 2015) and contributes to pacemaking. It has been shown that loss-of-function of HCN channel mutations is associated with sick sinus syndrome, which manifests with symptoms of bradycardia and conduction block (Schweizer et al., 2014; Verkerk and Wilders, 2014, 2015). However, the functional role of I_f in generating pacemaking action potentials of human SAN is less well-characterized as compared to that from small mammals. Limited data have shown that I_f in the human SAN cells has a smaller current density, more negative depolarised membrane potential of half maximal activation and slower activation rate as compared to the rabbit (Verkerk et al., 2007a,b, 2009b). All of these suggested a smaller I_f current during the diastolic depolarization phase, which may result in a slower heart rate. Indeed this is the case as shown in the present simulation study. In the Severi et al. model (Severi et al., 2012) with the rabbit-like I_f formulation, the measured pacemaking cycle length was 354.8 ms. However, when the rabbit-like I_f formulation was replaced by the human one, the pacemaking rate was slowed down and the pacemaking cycle length increased to 1,139.4 ms, greater than the intrinsic pacemaking cycle length of native human SAN cells [about 828 ± 21 ms (Verkerk et al., 2007b)]. Note that in the model, such a significant increase of the pacemaking CL from the one of rabbit SAN cells to the one close to human SAN cells was mainly attributable to a small I_f, as no change or negligible secondary changes of other ion channels were implemented. This suggests that I_f exerts a strong influence on pacemaker rhythm. Note that there is a marked difference in the pacemaking CL between the human-like model (1,139.4 ms) and native human SAN cells [about 828 ± 21 ms (Verkerk et al., 2007b)], which may be due to possible species differences in the properties of other membrane currents (Fabbri et al., 2017) and Ca^{2+} clock (Tsutsui et al., 2018). With the increase of I_f blocking, the pacemaking CL increased non-linearly in the model with either rabbit-like or human-like I_f formulations.

In simulations, the action of 100% I_f block abolished the pacemaking in the model with rabbit-like I_f formulations. This may over emphasize the role of I_f in the rabbit SAN pacemaking and is non-physiological. However, the focus of this study is on the action of small I_f block (i.e., <20%), mimicking the use of effect of ivabradine in practice, rather than on the action of large percentage of I_f block. With <50% I_f block, the increase in CL is about <30%, which is reasonably close to the experimental data observed in rabbit SAN cells when I_f is blocked by use of Cs^+ (Nikmaram et al., 1997).

Mechanism for the Action of Low Dose Ivabradine on Human SAN

Our theoretical and numerical simulation results have shown that a low level of I_f block, mimicking the clinical concentrations of ivabradine, produced a more marked effect in reducing the heart rate of the human-like I_f formulation SAN cell model than the rabbit-like I_f formulation SAN cell model. When the action of ACh (0.1 nM) was considered, there was a further reduction of sponteneous pacing rate (reduced upto by 27.3%), which is close to the effect of ivabradine at clinical concentration. Results from the Fabbri et al. model were similar, showing that these observations are model-independent. All these results suggest that a combined action of I_f reduction by ivabradine at clinical concentrations and ACh are attributable to the heart rate reduction as seen clinically (Camm and Lau, 2003; Doesch et al., 2007).

It is possible that ivabradine regulates the heart rate by a cross-talk between the membrane clock and Ca^{2+} clock *via* the electrogenic Na^+-Ca^{2+} exchangers (Yaniv et al., 2013). While the direct action of ivabradine on the intracellular Ca^{2+} handling is unclear, our simulation results showed that a 20% I_f reduction produced secondary modulations of other ionic currents (e.g., I_{NaCa}) and the intracellular Ca^{2+} handling, suggesting there

is a cross-talk between the membrane clock and Ca^{2+} clock in the late phase of the diastolic depolarization of the action potential (**Figures 4Bii–Eii**). All these illustrated that ivabradine affected the heart rate at clinical concentrations mainly through regulating membrane clock and Ca^{2+} clock, and combining with the action of ACh.

Limitations of the Study

Possible limitations of the Severi et al. model of the rabbit SAN cells have been well-discussed and documented (Severi et al., 2012). For example, as highlighted by Verkerk and Wilders (2014), the reversal potential of I_f in the Severi et al. model (−4.39 mV) was more positive than that experimentally reported (about −30 mV) (Difrancesco et al., 1986; Van Ginneken and Giles, 1991; Verkerk et al., 2009a), which is a limitation of the Severi et al. model, and therefore also of studies employing this model. However, we did not modify the I_f equation of the Severi et al. model for the following reasons: (1) the simulated I-V relationship data shown in (**Figure 1C**) lie within the range of experimental data, and I_f is very small when the voltage is more positive than −40 mV; (2) when the voltage is more positive than −30 mV, the activation of I_{CaL} is dominant, which contributes mainly to the upstroke phase (non-diastolic depolarization phase) of the action potential. Therefore, even if the reversal potential of I_f is changed from −30 mV to −4.39 mV, it has negligible effect on the diastolic depolarization of spontaneous action potentials. Moreover, in simulations in which the rabbit-like I_f was replaced by the human-like formulations in the Severi et al. model, the reversal potential of I_f used was −27.5 mV, close to the experimentally determined value of -22.1 ± 2.4 mV (Verkerk et al., 2007b).

Another potential limitation of the present study relates to modification of the Severi et al. model to incorporate the human I_f formulation developed by Fabbri et al. based on experimental data from human SAN cells. Due to lack of experimental data from human SAN cells, equations and parameters for other ion channels and transporters in the Severi et al. model were not updated. Note that experimental data on the Ca^{2+} clock of the human SAN became available recently (Tsutsui et al., 2018), which are not incorporated in the model yet. This may explain why the computed CL of the human-like SAN cell is greater than that of natural human SAN cells, and consequently the smaller effect of I_f blocking on the reduction of the heart rate the clinical data. In addition, the action of low dose ivabradine was simulated by considering its action on blocking I_f only, and did not incorporate its possible actions on I_{Kr} as seen in some experimental studies on ventricular cells/tissue at low dose (Melgari et al., 2015) or high doses (Lees-Miller et al., 2015). However, the present study deliberately focused on the difference in direct effects of ivabradine on I_f in the SAN cells between species (I_f in the rabbit SAN and in the human-like SAN). Whilst it is necessary to point out these potential limitations, nevertheless, the simulation data strongly supported the mechanism demonstrated by the theoretical analysis in showing the inverse correlation between I_{total} during the diastolic depolarization phase and the relative increase of the CL. Therefore, these limitations do not alter our major conclusion on the role of I_f block in modulating cardiac pacemaking activities in the human SAN by low concentrations of ivabradine.

CONCLUSION

An inverse correlation between the relative increase of CL and the amplitude of the total ion channel current during the diastolic depolarization phase has been observed. Both theoretical analysis and simulations have shown that a low level of I_f block (<20%) can produce a more marked reduction of in the pacemaking rate of the human-like SAN cell model than the rabbit-like one due to its smaller I_{total} during the diastolic depolarization phase. This was particularly the case when ACh actions were considered, which amplified the pacemaking cycle length prolongation. This study thus provides a mechanistic explanation into how a low level of I_f block by the clinical concentrations of ivabradine can effectively reduce the heart rate in humans but produce a small or negligible effect in the rabbit.

DATA AVAILABILITY STATEMENT

The original contributions presented in the study are included in the article/**Supplementary Material**, further inquiries can be directed to the corresponding author/s.

CODE AVAILABILITY STATEMENT

The code for the models employed is available on request to Henggui Zhang at henggui.zhang@manchester.ac.uk.

AUTHOR CONTRIBUTIONS

HZ and JH conceived the study. XB conducted simulation and data analysis. HZ and MB contributed to theoretical analysis. XB, KW, MB, JH, and HZ wrote the paper. All authors contributed to the article and approved the submitted version.

FUNDING

This work was supported by grants from the British Heart Foundation FS/14/5/30533, EPSRC (UK) (EP/J00958X/1; EP/I029826/1), Shenzhen Science and Technology Innovation Committee (JCYJ20151029173639477; JSGG20160229125049615), and Scientific research plan projects of Shaanxi Education Department (20JK0917). JH received a University of Bristol Research Fellowship.

ACKNOWLEDGMENTS

We are grateful to Dr. Severi's group for providing us the source code of the Severi et al. model.

SUPPLEMENTARY MATERIAL

The Supplementary Material for this article can be found online at: https://www.frontiersin.org/articles/10.3389/fphys.2021.582037/full#supplementary-material

REFERENCES

Accili, E. A., Robinson, R. B., and Difrancesco, D. (1997). Properties and modulation of I_f in newborn versus adult cardiac SA node. *Am. J. Physiol.* 272, H1549–H1552. doi: 10.1152/ajpheart.1997.272.3.H1549

Altomare, C., Terragni, B., Brioschi, C., Milanesi, R., Pagliuca, C., Viscomi, C., et al. (2003). Heteromeric HCN1-HCN4 channels: a comparison with native pacemaker channels from the rabbit sinoatrial node. *J. Physiol.* 549, 347–359. doi: 10.1113/jphysiol.2002.027698

Barbuti, A., Baruscotti, M., and Difrancesco, D. (2007). The pacemaker current: from basics to the clinics. *J. Cardiovasc. Electrophysiol.* 18, 342–347. doi: 10.1111/j.1540-8167.2006.00736.x

Baruscotti, M., Bianco, E., Bucchi, A., and Difrancesco, D. (2016). Current understanding of the pathophysiological mechanisms responsible for inappropriate sinus tachycardia: role of the I_f "funny" current. *J. Interv. Card Electrophysiol.* 46, 19–28. doi: 10.1007/s10840-015-0097-y

Baruscotti, M., Bucchi, A., and Difrancesco, D. (2005). Physiology and pharmacology of the cardiac pacemaker ("funny") current. *Pharmacol. Ther.* 107, 59–79. doi: 10.1016/j.pharmthera.2005.01.005

Baruscotti, M., Bucchi, A., Viscomi, C., Mandelli, G., Consalez, G., Gnecchi-Rusconi, T., et al. (2011). Deep bradycardia and heart block caused by inducible cardiac-specific knockout of the pacemaker channel gene *Hcn4*. *Proc. Natl. Acad. Sci. U. S. A.* 108, 1705–1710. doi: 10.1073/pnas.1010122108

Bohm, M., Robertson, M., Ford, I., Borer, J. S., Komajda, M., Kindermann, I., et al. (2015). Influence of cardiovascular and noncardiovascular co-morbidities on outcomes and treatment effect of heart rate reduction with ivabradine in stable heart failure (from the SHIFT trial). *Am. J. Cardiol.* 116, 1890–1897. doi: 10.1016/j.amjcard.2015.09.029

Bois, P., Bescond, J., Renaudon, B., and Lenfant, J. (1996). Mode of action of bradycardic agent, S 16257, on ionic currents of rabbit sinoatrial node cells. *Br. J. Pharmacol.* 118, 1051–1057. doi: 10.1111/j.1476-5381.1996.tb15505.x

Bois, P., Guinamard, R., Chemaly, A. E., Faivre, J. F., and Bescond, J. (2007). Molecular regulation and pharmacology of pacemaker channels. *Curr. Pharm. Des.* 13, 2338–2349. doi: 10.2174/138161207781368729

Boyett, M. R. (2009). "And the beat goes on." The cardiac conduction system: the wiring system of the heart. *Exp. Physiol.* 94, 1035–1049. doi: 10.1113/expphysiol.2009.046920

Boyett, M. R., Kodama, I., Honjo, H., Arai, A., Suzuki, R., and Toyama, J. (1995). Ionic basis of the chronotropic effect of acetylcholine on the rabbit sinoatrial node. *Cardiovasc. Res.* 29, 867–878. doi: 10.1016/S0008-6363(96)88625-1

Brioschi, C., Micheloni, S., Tellez, J. O., Pisoni, G., Longhi, R., Moroni, P., et al. (2009). Distribution of the pacemaker HCN4 channel mRNA and protein in the rabbit sinoatrial node. *J. Mol. Cell Cardiol.* 47, 221–227. doi: 10.1016/j.yjmcc.2009.04.009

Bucchi, A., Baruscotti, M., and Difrancesco, D. (2002). Current-dependent block of rabbit sino-atrial node I_f channels by ivabradine. *J. Gen. Physiol.* 120, 1–13. doi: 10.1085/jgp.20028593

Bucchi, A., Baruscotti, M., Nardini, M., Barbuti, A., Micheloni, S., Bolognesi, M., et al. (2013). Identification of the molecular site of ivabradine binding to HCN4 channels. *PLoS ONE* 8:e53132. doi: 10.1371/journal.pone.0053132

Bucchi, A., Baruscotti, M., Robinson, R. B., and Difrancesco, D. (2003). I_f-dependent modulation of pacemaker rate mediated by cAMP in the presence of ryanodine in rabbit sino-atrial node cells. *J. Mol. Cell Cardiol.* 35, 905–913. doi: 10.1016/S0022-2828(03)00150-0

Bucchi, A., Baruscotti, M., Robinson, R. B., and Difrancesco, D. (2007). Modulation of rate by autonomic agonists in SAN cells involves changes in diastolic depolarization and the pacemaker current. *J. Mol. Cell Cardiol.* 43, 39–48. doi: 10.1016/j.yjmcc.2007.04.017

Bucchi, A., Tognati, A., Milanesi, R., Baruscotti, M., and Difrancesco, D. (2006). Properties of ivabradine-induced block of HCN1 and HCN4 pacemaker channels. *J. Physiol.* 572, 335–346. doi: 10.1113/jphysiol.2005.100776

Camici, P. G., Gloekler, S., Levy, B. I., Skalidis, E., Tagliamonte, E., Vardas, P., et al. (2016). Ivabradine in chronic stable angina: effects by and beyond heart rate reduction. *Int. J. Cardiol.* 215, 1–6. doi: 10.1016/j.ijcard.2016.04.001

Camm, A. J., and Lau, C. P. (2003). Electrophysiological effects of a single intravenous administration of ivabradine (S 16257) in adult patients with normal baseline electrophysiology. *Drugs R D* 4, 83–89. doi: 10.2165/00126839-200304020-00001

Chandler, N. J., Greener, I. D., Tellez, J. O., Inada, S., Musa, H., Molenaar, P., et al. (2009). Molecular architecture of the human sinus node: insights into the function of the cardiac pacemaker. *Circulation* 119, 1562–1575. doi: 10.1161/CIRCULATIONAHA.108.804369

Choi, H. Y., Noh, Y. H., Cho, S. H., Ghim, J. L., Choe, S., Kim, U. J., et al. (2013). Evaluation of pharmacokinetic and pharmacodynamic profiles and tolerability after single (2.5, 5, or 10 mg) and repeated (2.5, 5, or 10 mg bid for 4.5 days) oral administration of ivabradine in healthy male Korean volunteers. *Clin. Ther.* 35, 819–835. doi: 10.1016/j.clinthera.2013.04.012

Craven, K. B., and Zagotta, W. N. (2006). CNG and HCN channels: two peas, one pod. *Annu. Rev. Physiol.* 68, 375–401. doi: 10.1146/annurev.physiol.68.040104.134728

Denyer, J. C., and Brown, H. F. (1990). Pacemaking in rabbit isolated sino-atrial node cells during Cs^+ block of the hyperpolarization-activated current i_f. *J. Physiol.* 429, 401–409. doi: 10.1113/jphysiol.1990.sp018264

Difrancesco, D. (1991). The contribution of the "pacemaker" current (if) to generation of spontaneous activity in rabbit sino-atrial node myocytes. *J. Physiol.* 434, 23–40. doi: 10.1113/jphysiol.1991.sp018457

Difrancesco, D. (2010). The role of the funny current in pacemaker activity. *Circ. Res.* 106, 434–446. doi: 10.1161/CIRCRESAHA.109.208041

Difrancesco, D., Ducouret, P., and Robinson, R. B. (1989). Muscarinic modulation of cardiac rate at low acetylcholine concentrations. *Science* 243, 669–671. doi: 10.1126/science.2916119

Difrancesco, D., Ferroni, A., Mazzanti, M., and Tromba, C. (1986). Properties of the hyperpolarizing-activated current (i_f) in cells isolated from the rabbit sino-atrial node. *J. Physiol.* 377, 61–88. doi: 10.1113/jphysiol.1986.sp016177

Difrancesco, D., and Noble, D. (2012). The funny current has a major pacemaking role in the sinus node. *Heart Rhythm* 9, 299–301. doi: 10.1016/j.hrthm.2011.09.021

Doesch, A. O., Celik, S., Ehlermann, P., Frankenstein, L., Zehelein, J., Koch, A., et al. (2007). Heart rate reduction after heart transplantation with beta-blocker versus the selective I_f channel antagonist ivabradine. *Transplantation* 84, 988–996. doi: 10.1097/01.tp.0000285265.86954.80

Fabbri, A., Fantini, M., Wilders, R., and Severi, S. (2017). Computational analysis of the human sinus node action potential: model development and effects of mutations. *J. Physiol.* 595, 2365–2396. doi: 10.1113/JP273259

Goethals, M., Raes, A., and Van Bogaert, P. P. (1993). Use-dependent block of the pacemaker current I(f) in rabbit sinoatrial node cells by zatebradine (UL-FS 49). On the mode of action of sinus node inhibitors. *Circulation* 88, 2389–2401. doi: 10.1161/01.CIR.88.5.2389

Hagiwara, N., and Irisawa, H. (1989). Modulation by intracellular Ca^{2+} of the hyperpolarization-activated inward current in rabbit single sino-atrial node cells. *J. Physiol.* 409, 121–141. doi: 10.1113/jphysiol.1989.sp017488

Hagiwara, N., Irisawa, H., and Kameyama, M. (1988). Contribution of two types of calcium currents to the pacemaker potentials of rabbit sino-atrial node cells. *J. Physiol.* 395, 233–253. doi: 10.1113/jphysiol.1988.sp016916

Herrmann, S., Stieber, J., Stockl, G., Hofmann, F., and Ludwig, A. (2007). HCN4 provides a "depolarization reserve" and is not required for heart rate acceleration in mice. *EMBO J.* 26, 4423–4432. doi: 10.1038/sj.emboj.7601868

Hoesl, E., Stieber, J., Herrmann, S., Feil, S., Tybl, E., Hofmann, F., et al. (2008). Tamoxifen-inducible gene deletion in the cardiac conduction system. *J. Mol. Cell Cardiol.* 45, 62–69. doi: 10.1016/j.yjmcc.2008.04.008

Irisawa, H., Brown, H. F., and Giles, W. (1993). Cardiac pacemaking in the sinoatrial node. *Physiol. Rev.* 73, 197–227. doi: 10.1152/physrev.1993.73.1.197

Jiang, J., Tian, L., Huang, Y., Li, Y., and Xu, L. (2013). Pharmacokinetic and safety profile of ivabradine in healthy Chinese men: a phase I, randomized, open-label, increasing single- and multiple-dose study. *Clin. Ther.* 35, 1933–1945. doi: 10.1016/j.clinthera.2013.10.007

Joannides, R., Moore, N., Iacob, M., Compagnon, P., Lerebours, G., Menard, J. F., et al. (2006). Comparative effects of ivabradine, a selective heart rate-lowering agent, and propranolol on systemic and cardiac haemodynamics at rest and during exercise. *Br. J. Clin. Pharmacol.* 61, 127–137. doi: 10.1111/j.1365-2125.2005.02544.x

Kozasa, Y., Nakashima, N., Ito, M., Ishikawa, T., Kimoto, H., Ushijima, K., et al. (2018). HCN4 pacemaker channels attenuate the parasympathetic response and stabilize the spontaneous firing of the sinoatrial node. *J. Physiol.* 596, 809–825. doi: 10.1113/JP275303

Lakatta, E. G., and Difrancesco, D. (2009). What keeps us ticking: a funny current, a calcium clock, or both? *J. Mol. Cell Cardiol.* 47, 157–170. doi: 10.1016/j.yjmcc.2009.03.022

Lakatta, E. G., Maltsev, V. A., and Vinogradova, T. M. (2010). A coupled SYSTEM of intracellular Ca^{2+} clocks and surface membrane voltage clocks controls the timekeeping mechanism of the heart's pacemaker. *Circ. Res.* 106, 659–673. doi: 10.1161/CIRCRESAHA.109.206078

Lees-Miller, J. P., Guo, J., Wang, Y., Perissinotti, L. L., Noskov, S. Y., and Duff, H. J. (2015). Ivabradine prolongs phase 3 of cardiac repolarization and blocks the hERG1 (KCNH2) current over a concentration-range overlapping with that required to block HCN4. *J. Mol. Cell Cardiol.* 85, 71–78. doi: 10.1016/j.yjmcc.2015.05.009

Li, N., Csepe, T. A., Hansen, B. J., Dobrzynski, H., Higgins, R. S., Kilic, A., et al. (2015). Molecular mapping of sinoatrial node HCN channel expression in the human heart. *Circ. Arrhythm Electrophysiol.* 8, 1219–1227. doi: 10.1161/CIRCEP.115.003070

Liu, J., Noble, P. J., Xiao, G., Abdelrahman, M., Dobrzynski, H., Boyett, M. R., et al. (2008). Role of pacemaking current in cardiac nodes: insights from a comparative study of sinoatrial node and atrioventricular node. *Prog. Biophys. Mol. Biol.* 96, 294–304. doi: 10.1016/j.pbiomolbio.2007.07.009

Madle, A., Linhartova, K., and Koza, J. (2001). Effects of the T-type calcium channel blockade with oral mibefradil on the electrophysiologic properties of the human heart. *Med. Sci. Monit.* 7, 74–77.

Maltsev, V. A., and Lakatta, E. G. (2008). Dynamic interactions of an intracellular Ca^{2+} clock and membrane ion channel clock underlie robust initiation and regulation of cardiac pacemaker function. *Cardiovasc. Res.* 77, 274–284. doi: 10.1093/cvr/cvm058

Maltsev, V. A., and Lakatta, E. G. (2010). Funny current provides a relatively modest contribution to spontaneous beating rate regulation of human and rabbit sinoatrial node cells. *J. Mol. Cell Cardiol.* 48, 804–806. doi: 10.1016/j.yjmcc.2009.12.009

Mangoni, M. E., and Nargeot, J. (2008). Genesis and regulation of the heart automaticity. *Physiol. Rev.* 88, 919–982. doi: 10.1152/physrev.00018.2007

Melgari, D., Brack, K. E., Zhang, C., Zhang, Y., El Harchi, A., Mitcheson, J. S., et al. (2015). hERG potassium channel blockade by the HCN channel inhibitor bradycardic agent ivabradine. *J. Am. Heart Assoc.* 4:1813. doi: 10.1161/JAHA.115.001813

Monfredi, O., Lyashkov, A. E., Johnsen, A. B., Inada, S., Schneider, H., Wang, R., et al. (2014). Biophysical characterization of the underappreciated and important relationship between heart rate variability and heart rate. *Hypertension* 64, 1334–1343. doi: 10.1161/HYPERTENSIONAHA.114.03782

Niccoli, G., Borovac, J. A., Vetrugno, V., Camici, P. G., and Crea, F. (2017). Ivabradine in acute coronary syndromes: protection beyond heart rate lowering. *Int. J. Cardiol.* 236, 107–112. doi: 10.1016/j.ijcard.2017.02.046

Nikmaram, M. R., Boyett, M. R., Kodama, I., Suzuki, R., and Honjo, H. (1997). Variation in effects of Cs^{+}, UL-FS-49, and ZD-7288 within sinoatrial node. *Am. J. Physiol.* 272, H2782–H2792. doi: 10.1152/ajpheart.1997.272.6.H2782

Ravagli, E., Bucchi, A., Bartolucci, C., Paina, M., Baruscotti, M., Difrancesco, D., et al. (2016). Cell-specific Dynamic Clamp analysis of the role of funny I_f current in cardiac pacemaking. *Prog. Biophys. Mol. Biol.* 120, 50–66. doi: 10.1016/j.pbiomolbio.2015.12.004

Rocchetti, M., Malfatto, G., Lombardi, F., and Zaza, A. (2000). Role of the input/output relation of sinoatrial myocytes in cholinergic modulation of heart rate variability. *J. Cardiovasc. Electrophysiol.* 11, 522–530. doi: 10.1111/j.1540-8167.2000.tb00005.x

Schweizer, P. A., Schroter, J., Greiner, S., Haas, J., Yampolsky, P., Mereles, D., et al. (2014). The symptom complex of familial sinus node dysfunction and myocardial noncompaction is associated with mutations in the HCN4 channel. *J. Am. Coll. Cardiol.* 64, 757–767. doi: 10.1016/j.jacc.2014.06.1155

Severi, S., Fantini, M., Charawi, L. A., and Difrancesco, D. (2012). An updated computational model of rabbit sinoatrial action potential to investigate the mechanisms of heart rate modulation. *J. Physiol.* 590, 4483–4499. doi: 10.1113/jphysiol.2012.229435

Takeda, K., Yamagishi, R., Masumiya, H., Tanaka, H., and Shigenobu, K. (2004). Effect of cilnidipine on L- and T-type calcium currents in guinea pig ventricle and action potential in rabbit sinoatrial node. *J. Pharmacol. Sci.* 95, 398–401. doi: 10.1254/jphs.SCJ04001X

Tardif, J. C., Ford, I., Tendera, M., Bourassa, M. G., Fox, K., and Investigators, I. (2005). Efficacy of ivabradine, a new selective I_f inhibitor, compared with atenolol in patients with chronic stable angina. *Eur. Heart J.* 26, 2529–2536. doi: 10.1093/eurheartj/ehi586

Thollon, C., Bedut, S., Villeneuve, N., Coge, F., Piffard, L., Guillaumin, J. P., et al. (2007). Use-dependent inhibition of hHCN4 by ivabradine and relationship with reduction in pacemaker activity. *Br. J. Pharmacol.* 150, 37–46. doi: 10.1038/sj.bjp.0706940

Thollon, C., Cambarrat, C., Vian, J., Prost, J. F., Peglion, J. L., and Vilaine, J. P. (1994). Electrophysiological effects of S 16257, a novel sino-atrial node modulator, on rabbit and guinea-pig cardiac preparations: comparison with UL-FS 49. *Br. J. Pharmacol.* 112, 37–42. doi: 10.1111/j.1476-5381.1994.tb13025.x

Tsutsui, K., Monfredi, O. J., Sirenko-Tagirova, S. G., Maltseva, L. A., Bychkov, R., Kim, M. S., et al. (2018). A coupled-clock system drives the automaticity of human sinoatrial nodal pacemaker cells. *Sci. Signal* 11:aap7608. doi: 10.1126/scisignal.aap7608

Van Ginneken, A. C., and Giles, W. (1991). Voltage clamp measurements of the hyperpolarization-activated inward current I(f) in single cells from rabbit sino-atrial node. *J. Physiol.* 434, 57–83. doi: 10.1113/jphysiol.1991.sp018459

Verkerk, A. O., Den Ruijter, H. M., Bourier, J., Boukens, B. J., Brouwer, I. A., Wilders, R., et al. (2009a). Dietary fish oil reduces pacemaker current and heart rate in rabbit. *Heart Rhythm.* 6, 1485–1492. doi: 10.1016/j.hrthm.2009.07.024

Verkerk, A. O., Van Borren, M. M., Peters, R. J., Broekhuis, E., Lam, K. Y., Coronel, R., et al. (2007a). Single cells isolated from human sinoatrial node: action potentials and numerical reconstruction of pacemaker current. *Conf. Proc. IEEE Eng. Med. Biol. Soc.* 2007, 904–907. doi: 10.1109/IEMBS.2007.4352437

Verkerk, A. O., Van Ginneken, A. C., and Wilders, R. (2009b). Pacemaker activity of the human sinoatrial node: role of the hyperpolarization-activated current, I_f. *Int. J. Cardiol.* 132, 318–336. doi: 10.1016/j.ijcard.2008.12.196

Verkerk, A. O., and Wilders, R. (2010). Relative importance of funny current in human versus rabbit sinoatrial node. *J. Mol. Cell Cardiol.* 48, 799–801. doi: 10.1016/j.yjmcc.2009.09.020

Verkerk, A. O., and Wilders, R. (2014). Pacemaker activity of the human sinoatrial node: effects of HCN4 mutations on the hyperpolarization-activated current. *Europace* 16, 384–395. doi: 10.1093/europace/eut348

Verkerk, A. O., and Wilders, R. (2015). Pacemaker activity of the human sinoatrial node: an update on the effects of mutations in HCN4 on the hyperpolarization-activated current. *Int. J. Mol. Sci.* 16, 3071–3094. doi: 10.3390/ijms16023071

Verkerk, A. O., Wilders, R., Van Borren, M. M. G. J., Peters, R. J. G., Broekhuis, E., Lam, K., et al. (2007b). Pacemaker current (I_f) in the human sinoatrial node. *Eur. Heart J.* 28, 2472–2478. doi: 10.1093/eurheartj/ehm339

Voigt, N., Abu-Taha, I., Heijman, J., and Dobrev, D. (2014). Constitutive activity of the acetylcholine-activated potassium current $I_{K,ACh}$ in cardiomyocytes. *Adv. Pharmacol.* 70, 393–409. doi: 10.1016/B978-0-12-417197-8.00013-4

Winter, J., and Shattock, M. J. (2016). Geometrical considerations in cardiac electrophysiology and arrhythmogenesis. *Europace* 18, 320–331. doi: 10.1093/europace/euv307

Yancy, C. W., Jessup, M., Bozkurt, B., Butler, J., Casey, D. E. Jr., Colvin, M. M., et al. (2016). 2016 ACC/AHA/HFSA focused update on new pharmacological therapy for heart failure: an update of the 2013 ACCF/AHA guideline for the management of heart failure: a report of the American College of Cardiology/American Heart Association Task Force on Clinical Practice Guidelines and the Heart Failure Society of America. *J. Am. Coll. Cardiol.* 68, 1476–1488. doi: 10.1016/j.jacc.2016.05.011

Yaniv, Y., Maltsev, V. A., Ziman, B. D., Spurgeon, H. A., and Lakatta, E. G. (2012). The "funny" current (I_f) inhibition by ivabradine at membrane potentials encompassing spontaneous depolarization in pacemaker cells. *Molecules* 17, 8241–8254. doi: 10.3390/molecules17078241

Yaniv, Y., Sirenko, S., Ziman, B. D., Spurgeon, H. A., Maltsev, V. A., and Lakatta, E. G. (2013). New evidence for coupled clock regulation of the normal automaticity of sinoatrial nodal pacemaker cells: bradycardic effects of ivabradine are linked to suppression of intracellular Ca^{2+} cycling. *J. Mol. Cell Cardiol.* 62, 80–89. doi: 10.1016/j.yjmcc.2013.04.026

Yuan, Y., Bai, X., Luo, C., Wang, K., and Zhang, H. (2015). The virtual heart as a platform for screening drug cardiotoxicity. *Br. J. Pharmacol.* 172, 5531–5547. doi: 10.1111/bph.12996

Zaza, A. (2016). Electrophysiology meets geometry. *Europace* 18:317. doi: 10.1093/europace/euv378

Zaza, A., and Lombardi, F. (2001). Autonomic indexes based on the analysis of heart rate variability: a view from the sinus node. *Cardiovasc. Res.* 50, 434–442. doi: 10.1016/S0008-6363(01)00240-1

Zaza, A., Robinson, R. B., and Difrancesco, D. (1996). Basal responses of the L-type Ca^{2+} and hyperpolarization-activated currents to autonomic agonists in the rabbit sino-atrial node. *J. Physiol.* 491, 347–355. doi: 10.1113/jphysiol.1996.sp021220

Conflict of Interest: The authors declare that the research was conducted in the absence of any commercial or financial relationships that could be construed as a potential conflict of interest.

Publisher's Note: All claims expressed in this article are solely those of the authors and do not necessarily represent those of their affiliated organizations, or those of the publisher, the editors and the reviewers. Any product that may be evaluated in this article, or claim that may be made by its manufacturer, is not guaranteed or endorsed by the publisher.